UCRL-16524

University of California

Ernest O. Lawrence Radiation Laboratory

PROPERTIES OF LIQUID HELIUM-THREE
IN THE TWO-BODY CORRELATION APPROXIMATION. I

Berkeley, California

Phys. Review

UCRL-16524

UNIVERSITY OF CALIFORNIA

Lawrence Radiation Laboratory
Berkeley, California

AEC Contract No. W-7405-eng-48

PROPERTIES OF LIQUID HELIUM-THREE IN THE TWO-BODY CORRELATION APPROXIMATION. I

Donald E. Beck and Andrew M. Sessler

November 17, 1965

UCRL-16524

PROPERTIES OF LIQUID HELIUM-THREE IN THE TWO-BODY CORRELATION APPROXIMATION. I*†

Donald E. Beck

Department of Physics
University of California-San Diego
La Jolla, California

and

Andrew M. Sessler

Lawrence Radiation Laboratory
University of California
Berkeley, California

November 17, 1965

ABSTRACT

This is the first of two papers in which the low-temperature properties of liquid He^3 are to be calculated in the thermodynamically consistent "T-matrix" approximation. The set of coupled integral equations which are to be solved is exhibited in Part A of this paper. Part B of this paper is devoted to a preliminary, zero-temperature calculation which employs the additional approximations of using separable potentials and a noninteracting spectral function to define the interaction of two particles in the medium: the $\langle T \rangle_0$ approximation. In this approximation we obtain a spectral function for the quasi particles which we expect to display general features in common with those of the actual spectral function. Using this spectral function, we calculate the thermodynamic properties of the system and find that they compare favorably to those obtained in other calculations.

type of system has been the "T-matrix" approximation,[3,8,9] which--in general terms--is an approximation that includes only effects arising from the explicit correlation of two particles.[10] Baym[11] has derived a criterion which any approximation must satisfy if it is to give self-consistent thermodynamics; he has shown that the "T-matrix" approximation satisfies the criterion.

This is the first of two papers concerning the solution of the coupled integral equations of the thermodynamically consistent T-matrix (TCTM) approximation. In the second paper of this series our program of obtaining the low-temperature properties of liquid He^3 within the framework of this approximation is accomplished.

Part A of this paper is devoted to exhibiting the coupled-integral equations of the TCTM approximation; here a brief discussion of the temperature-dependent Green's function formalism is also given. In Part B of this paper we make further approximations requisite for the preliminary calculation, which forms the main body of the paper. The coupled integral equations, defined in Part A, are simplified and decoupled by replacing the spectral functions in the T matrix by non-interacting spectral functions. The resulting T_0 matrix retains the essential interaction features exhibited by a zero-temperature system of interacting fermions; however, because of this decoupling our approximation is not thermodynamically consistent. This undesirable feature is a property shared by most other calculations to date (see Section VI.1); however, this approximation has the interesting property

(not shared by the other approximations) of yielding a spectral function with a width.

An additional approximation we make to obtain a manageable set of equations is that we use a finite sum of separable potentials to represent the interaction between two He^3 atoms. This approximation does not affect the thermodynamic consistency, but it may be a poor representation of the actual two-body interaction.

Section IV is devoted to developing the two-body interaction for particles in the medium; the T_0 matrix. In Section V we calculate the spectral function using this interaction and, since the modification of the two-body interaction due to statistics of the medium is well represented, we expect that our spectral function displays general features in common with that of the actual spectral function.

Because of the approximations for the interaction we would not expect the properties of liquid He^3 to be predicted with great accuracy. Nevertheless, in Section VI we calculate the ground-state properties and compare them both with experiment and with other calculations. The results of this comparison are summarized in Table I; the quantitative agreement with experiment is not impressive,[10] but as good as that of other approximations, and we may expect improvement in this comparison from the complete calculation.

Part A. T-Matrix (Two-Body Correlation) Approximation

II. GREEN'S FUNCTION FORMALISM

In this section it is shown that the thermodynamic properties of a system of interacting fermions may be evaluated in terms of the average energy, E, and number, N . The formalism of Martin and Schwinger[2,9] is summarized so as to clearly define the notation, and the formulae for E and N are presented in terms of calculable microscopic quantities.

1. Definition of the Problem; Thermodynamics

One assumes that the interaction in this system can be described by an instantaneous two-body Hamiltonian,[12]

$$H(t) = \frac{1}{2m}\int \nabla \psi^{\dagger}(\underset{\sim}{r},t)\nabla \psi(\underset{\sim}{r},t)d\underset{\sim}{r} + \frac{1}{2}\int \psi^{\dagger}(\underset{\sim}{r},t)\,\psi^{\dagger}(\underset{\sim}{r}',t)\,v(\underset{\sim}{r}-\underset{\sim}{r}')\,\psi(\underset{\sim}{r}',t)\,\psi(\underset{\sim}{r},t)d\underset{\sim}{r}\,d\underset{\sim}{r}' , \tag{1}$$

where $\psi^{\dagger}(\underset{\sim}{r},t)$ and $\psi(\underset{\sim}{r},t)$ are the particle creation and annihilation operators in the second-quantization Heisenberg representation; in this and subsequent expressions the coordinate $\underset{\sim}{r}$ contains the internal spin variables. In the same representation, the number operator is

$$N(t) = \int \psi^{\dagger}(\underset{\sim}{r},t)\,\psi(\underset{\sim}{r},t)d\underset{\sim}{r} . \tag{2}$$

The creation and annihilation operators satisfy the anticommutation relations

$$\{ \psi(\underset{\sim}{r},t), \psi(\underset{\sim}{r}',t) \} = 0 ,$$

$$\{ \psi(\underset{\sim}{r},t), \psi^{\dagger}(\underset{\sim}{r}',t) \} = \delta(\underset{\sim}{r} - \underset{\sim}{r}') . \tag{3}$$

Puff[9] employs a modified Heisenberg representation where the time development of an operator $X(t)$ is given by

$$X(t) = e^{i\mathcal{H}t} X(0) e^{-i\mathcal{H}t} , \tag{4}$$

with

$$\mathcal{H}(t) = H(t) - \mu N(t) , \tag{5}$$

and where μ is the chemical potential.

In order to describe the macroscopic behavior of the system, one evaluates the expectation value of operators over the grand-canonical ensemble.[13] Thus for an operator X, MS defines

$$\langle X \rangle^{\mu,\beta} = Z^{-1} \operatorname{tr} [e^{-\beta\mathcal{H}} X] . \tag{6}$$

where tr denotes the trace of the matrix is to be taken, and Z is the grand-canonical partition function,

$$Z = \operatorname{tr}[e^{-\beta\mathcal{H}}] . \tag{7}$$

The thermodynamic state of the system is defined by μ and β, the inverse temperature measured in energy units; i.e., $\beta = 1/\kappa T$, where κ is Boltzman's constant. It is well known[14] that all the equilibrium thermodynamic properties can be obtained from the grand partition function.

For a given μ and β one can compute this function[15] if he knows

$$E = \langle H \rangle^{\mu,\beta} \tag{8}$$

and

$$N = \langle N \rangle^{\mu,\beta} , \tag{9}$$

as can be seen by the following argument: At zero temperature the pressure P is, according to its definition,

$$P = -\left(\frac{\partial E}{\partial \mathcal{V}}\right)_N = \left(\frac{N}{\mathcal{V}}\right)^2 \frac{\partial}{\partial \left(\frac{N}{\mathcal{V}}\right)} \left(\frac{E}{N}\right) , \tag{10}$$

where $\mathcal{V}$ is the volume of the system. For a normal system of fermions at zero temperature the Hugenholtz-Van Hove theorem[16] states

$$\left(\frac{\partial E}{\partial N}\right)_{\mathcal{V}} = \mu , \tag{11}$$

which has the consequence, for a large system, that

$$\mu = \frac{E}{N} + \left(\frac{N}{\mathcal{V}}\right) \frac{\partial}{\partial \left(\frac{N}{\mathcal{V}}\right)} \left(\frac{E}{N}\right) . \tag{12}$$

The grand-canonical partition function is related to the pressure by[14]

$$Z^{\mu,\beta} = e^{\beta P \mathcal{V}} . \tag{13}$$

Differentiating the logarithm of Z with respect to μ at fixed β and $\mathcal{V}$, one obtains a relation between $\partial P/\partial \mu$ and $\langle N/\mathcal{V} \rangle^{\mu,\beta}$,[15] and, similarly, differentiating the logarithm with respect to β at fixed μ and $\mathcal{V}$; one obtains a relation between $\partial P/\partial \beta$ and $\langle H/\mathcal{V} \rangle^{\mu,\beta}$. These relations can be integrated to give $P^{\mu,\beta}$, and hence one can compute all the properties of the system, if he has E and N (Eqs. 8 and 9).

2. Microscopic Theory

Equations (8) and (9) may be evaluated from a microscopic theory by using Green's functions. The one-particle Green's functions is[17]

$$G(11') = -i \langle T\big(\psi(1)\, \psi^{\dagger}(1')\big)\rangle^{\mu,\beta} , \tag{14}$$

and the two-particle function is given by

$$G_2(12;1'2') = (-i)^2 \langle T\big(\psi(1)\, \psi(2)\, \psi^{\dagger}(2')\, \psi^{\dagger}(1')\big)\rangle^{\mu,\beta} ;$$

in these functions T is the Wick time-ordering operator.

Using (4) to define G for complex values of its time arguments, in the interval

$$0 \leq i t \leq \beta ,$$

and defining the time ordering in this interval by

$$T(\psi(1)\, \psi^{\dagger}(1')) = \psi(1)\, \psi^{\dagger}(1') \quad \text{for } i t_1 > i t'_1 ,$$

$$= -\psi^{\dagger}(1')\, \psi(1) \quad \text{for } i t_1 < i t'_1 ,$$

one can use the cyclic property of the trace to obtain the boundary condition

$$G(11')\Big|_{t_1=0} = -G(11')\Big|_{t_1=-i\beta} . \tag{15}$$

The Hamiltonian, Eq. (1), is translationally invariant in space and time (we assume an infinite system so there are no boundary effects), and consequently

$$G(11') = G(\underset{\sim}{r},t) ,$$

where $\underset{\sim}{r} = \underset{\sim}{r}_1 - \underset{\sim}{r}_{1'}$, $t = t_1 - t_{1'}$.

Introducing a "spectral function," $A(\underset{\sim}{p},\omega)$, for G , and performing Fourier integral transforms with respect to the space components of G , and a Fourier series analysis with respect to the time component, MS obtain

$$G(\underset{\sim}{p},z_\nu) = \int \frac{d\omega}{2\pi} \frac{A(\underset{\sim}{p},\omega)}{z_\nu - \omega} ,$$

where $z_\nu = \pi\nu/(-i\beta)$. Define the analytic function

$$G(\underset{\sim}{p},z) = \int \frac{d\omega}{2\pi} \frac{A(\underset{\sim}{p},\omega)}{z - \omega} \tag{16}$$

for all nonreal z , by analytically continuing from the points z_ν . The unique continuation has been shown by Baym and Mermin[18] to be that which has no essential singularity at $|z| = \infty$. Thus $G(\underset{\sim}{p},z)$ is a function which is analytic in the whole complex z plane with the exception of the real axis, while $A(\underset{\sim}{p},\omega)$ --a real positive function-- is given by the discontinuity of G across the real axis,

$$A(\underset{\sim}{p},\omega) = i[G(\underset{\sim}{p},\omega + i\epsilon) - G(\underset{\sim}{p},\omega - i\epsilon)] . \tag{17}$$

Using the anticommutation relation, (3), one can easily obtain the sum rule:

$$\int_{-\infty}^{+\infty} \frac{d\omega}{2\pi} A(\underset{\sim}{p},\omega) = 1 . \tag{18}$$

For a given approximation the anticommutation relation may not exist or may not be in a convenient form to obtain this sum rule for $A(\underset{\sim}{p},\omega)$. In this case we need to know the properties that must be satisfied by G to ensure the sum rule. The Herglotz theorem[19] (of the theory of analytic functions) gives the necessary and sufficient conditions on $G(\underset{\sim}{p},z)$: If $G(\underset{\sim}{p},z)$ is analytic in the upper half plane, $\text{Im } z > 0$, and if in this half plane $\text{Im } G \leqslant 0$ and $\lim_{|z|\to\infty} z\, G(z) = 1$, then the sum rule, (18), holds.

In Section II.1 it was shown that one needs the two quantities E and N , (Eqs. 8 and 9), in order to obtain the equilibrium thermodynamic properties of the system. These quantities can be expressed in terms of the spectral function $A(\underset{\sim}{p},\omega)$. The number density operator for the system is , (2),

$$n(\underset{\sim}{r},t) = \psi^{\dagger}(\underset{\sim}{r},t)\, \psi(\underset{\sim}{r},t) ,$$

so that, from (15) and (16),

$$\langle\, n(\underset{\sim}{r},t)\, \rangle = \int \frac{d\omega}{2\pi} \int \frac{d\underset{\sim}{p}}{(2\pi)^3}\, A(\underset{\sim}{p},\omega)\, f(\omega) ,$$

where

$$f(\omega) = [e^{\beta\omega} + 1]^{-1}$$

is the usual fermion statistical factor. Since the system is isotropic, $\langle n(\underset{\sim}{r},t)\rangle$ is independent of $\underset{\sim}{r}$ and t and it follows that

$$\left\langle \frac{N}{\mathcal{V}} \right\rangle^{\mu,\beta} = \int \frac{d\omega}{2\pi} \int \frac{d\underset{\sim}{p}}{(2\pi)^3}\, A(\underset{\sim}{p},\omega)\, f(\omega) ; \qquad (19)$$

for our system N and $\mathcal{V}$ go to infinity in a manner such that the ratio $(N/\mathcal{V})$ remains finite. Similarly, the energy density is given by

$$\left\langle \frac{H}{\mathcal{V}} \right\rangle^{\mu,\beta} = \int \frac{d\omega}{2\pi} \int \frac{d\underset{\sim}{p}}{(2\pi)^3} \frac{\omega + \frac{p^2}{2m} - \mu}{2} A(\underset{\sim}{p},\omega) f(\omega) \ . \quad (20)$$

The equation of motion for G is

$$(i \frac{\partial}{\partial t_1} + \frac{\nabla_1^2}{2m} + \mu)\ G(11') + i\int d\underset{\sim}{r}_2\ v(\underset{\sim}{r}_1 - \underset{\sim}{r}_2) G_2(12;1'2^+)\Big|_{t_2=t_1} = \delta(1 - 1'), \quad (21)$$

where $(2^+) = (\underset{\sim}{r}_2,\ t_2 + 0^+)$. One sees that this equation involves G_2, and the equation of motion for G_n would involve G_{n-1} and G_{n+1}. Therefore, one has to solve an infinite set of coupled differential-integral equations in order to obtain G.

It is useful to introduce--following MS--the "self-energy" operator, Σ, which is defined so that

$$(i \frac{\partial}{\partial t_1} + \frac{\nabla_1^2}{2m} + \mu)G(11') - \int_0^{-i\beta} d\bar{1}\ \Sigma(1\bar{1})\ G(\bar{1}1') = \delta(1 - 1') \ . \quad (22)$$

One can show[15] that Σ satisfies the same boundary conditions as G. One defines a "spectral function" for Σ,

$$\Gamma(\underset{\sim}{p},\omega) = i\ [\ \Sigma(\underset{\sim}{p},\ \omega + i\epsilon) - \Sigma(\underset{\sim}{p},\ \omega - i\epsilon)]\ , \quad (23)$$

and consequently

$$\Sigma(\underset{\sim}{p},z) = \int_{-\infty}^{+\infty} \frac{d\omega}{2\pi} \frac{\Gamma(\underset{\sim}{p},\omega)}{z - \omega} + \Sigma_0(\underset{\sim}{p}) ,$$

where $\Sigma_0(\underset{\sim}{p})$ is a real valued function of $\underset{\sim}{p}$ only. Here allowance is made for the possibility[20] that

$$\lim_{|z|\to\infty} \Sigma(z) = \Sigma_0 .$$

When a Fourier integral transform is performed on the coordinate variables and a Fourier series analysis of the time variable, (22) becomes

$$[\, z - \frac{p^2}{2m} + \mu - \Sigma(\underset{\sim}{p},z)]G(\underset{\sim}{p},z) = 1 , \qquad (24)$$

which, combined with (17) and (23), yields

$$A(\underset{\sim}{p},z) = \Gamma(\underset{\sim}{p},\omega) \left[\left(\omega - \frac{p^2}{2m} + \mu - \mathrm{Re}\ \Sigma(\underset{\sim}{p},\omega) \right)^2 + \frac{\Gamma(\underset{\sim}{p},\omega)^2}{4} \right]^{-1} . \qquad (25)$$

III. THE THERMODYNAMICALLY CONSISTENT T-MATRIX APPROXIMATION

1. Motivation and Specification of the Approximation

In Section II we discussed the infinite set of coupled integro-differential equations [the first of which is given by (21)], which need to be solved to obtain G. One cannot hope to solve this set of coupled equations exactly; some approximations must be made.

For short-range forces with strong repulsion a useful approximation which has been widely employed is the T-matrix approximation.[3,8,9] This is an approximation for G_3 which neglects the correlation of a single particle with a highly correlated pair. Formally, one takes[9]

$$G_3(123;\, 1'2'3') = G(13')\, G_2(23;\, 1'2') + G(11')\, G_2(23;\, 2'3') - G(12')\, G_2(23;\, 1'3') ,$$

which gives

$$G_2(12;\, 1'2') = [G(11')\, G(22') - G(12')\, G(21')] + \frac{i}{2} \int_0^{-i\beta} d\bar{1}\, d\bar{2}\, [G^o(1\bar{1})\, G(2\bar{2}) - G(1\bar{1})\, G^o(2\bar{2})] \times V(\bar{1} - \bar{2})\, G_2(\bar{1}\,\bar{2};\, 1'2') , \qquad (26)$$

where G^o is the solution of (21) without the interaction term, and

$$V(1 - 2) = v(\underset{\sim}{r}_1 - \underset{\sim}{r}_2)\, \delta(t_1 - t_2) .$$

An important further consideration in making approximations is thermodynamic consistency. If the approximations do not satisfy certain consistency requirements, one has no guarantee that the thermodynamic quantities obtained are consistent. At zero temperature if the results are such that the Hugenholtz-Van Hove theorem, (11), is not satisfied then one does not know how to determine the pressure uniquely. The situation is just as serious at a temperature because the pressure, $P^{\mu\beta}$, obtained by two different integration paths--using the relations between $\partial P/\partial\mu$ and $\langle N/\mathcal{V}\rangle^{\mu\beta}$, and $\partial P/\partial\beta$ and $\langle H/\mathcal{V}\rangle^{\mu,\beta}$ --discussed at the end of Section II.1--may not be unique. Still a third result for the pressure might be found by integrating the expectation value of the potential energy with respect to the coupling constant.[15]

As might be expected, the demand that an approximation lead to a single-particle Green's function such that the thermodynamic results are consistent places strong restrictions on the possible class of approximations. Baym[11] has used functional derivative techniques to derive a criterion for approximating the single-particle Green's function and has proven that approximations which satisfy this criterion produce a consistent picture. His criterion is that there must exist a "closed" functional Φ of G and the potential, V, such that

$$\Sigma(11') = \frac{\delta \Phi}{\delta G(11')} , \qquad (27)$$

where the self-energy, Σ, is to be considered as a functional of G and V. Here a "closed" functional means one in which all internal

variables are integrated, or, in terms of diagrams, no particle lines enter or leave the diagram. In terms of diagrams, the differentiation of Eq. (27), means plucking out one of the particle lines, as is detailed in Fig. 1.

The approximation (26) does not satisfy Baym's criterion; however, Baym[11] has shown that the approximation

$$G_2(12;\,1'2') = [G(11')\,G(22') - G(12')\,G(21')] + i\int_0^{-i\beta} d\bar{1}\,d\bar{2}\,G(1\bar{1})\,G(2\bar{2})\,V(\bar{1}-\bar{2})\,G_2(\bar{1}\,\bar{2};\,12) \tag{28}$$

does satisfy his criterion.

2. Formal Development of the TCTM Approximation

We take Eq. (28) as the basic equation of our thermodynamically consistent T-matrix (TCTM) approximation. If we define the T matrix by the integral equation

$$\langle\, 12 \mid T \mid 1'2' \,\rangle = V(1-2)\,\delta(1-1')\,\delta(2-2') + i\int_0^{-i\beta} d\bar{1}\,d\bar{2}\,\langle\, 12 \mid T \mid \bar{1}\,\bar{2} \,\rangle\, G(\bar{1}1')\,G(\bar{2}2')\,V(1'-2'), \tag{29}$$

the approximation, (28), becomes

$$V(1-2)\,G_2(12;\,1'2') = \int_0^{-i\beta} d\bar{1}\,d\bar{2}\,\langle\, 12 \mid T \mid \bar{1}\,\bar{2} \,\rangle \times [G(\bar{1}1')\,G(\bar{2}2') - G(\bar{2}1')\,G(\bar{1}2')], \tag{30}$$

and from (21) and (22) we have

$$\Sigma(11') = -i \int_0^{-i\beta} d2\, d\bar{2} \left[\langle\, 12 \,|T|\, 1'\bar{2} \,\rangle - \langle\, 12 \,|T|\, \bar{2}1' \,\rangle \right] G(\bar{2}2^+) \,. \tag{31}$$

Examining the structure of $\langle |T| \rangle$, one sees that it satisfies the same boundary condition as $G(t_1 - t_{1'})G(t_1 - t_{1'})$:

$$T(t_1 - t_{1'})\Big|_{t_1=0} = T(t_1 - t_{1'})\Big|_{t_1=-i\beta} \,.$$

One can express $T(t_1 - t_{1'})$ as a Fourier series with coefficients $T(z_\nu)$, where $z_\nu = \pi\nu/(-i\beta)$ and ν runs over all even integers. Analytically continuing to all z, and performing Fourier integral transformations with respect to the center of mass and relative coordinates (see Chapter 13 of Kadanoff and Baym[15]), one obtains

$$\langle\, \underset{\sim}{p} \,|T(\underset{\sim}{P},z)|\, \underset{\sim}{p}' \,\rangle = v(\underset{\sim}{p} - \underset{\sim}{p}') + \int \frac{d\bar{\underset{\sim}{p}}}{(2\pi)^3} \langle\, \underset{\sim}{p} \,|T(\underset{\sim}{P},z)|\, \bar{\underset{\sim}{p}} \,\rangle \Lambda(\underset{\sim}{P},\bar{\underset{\sim}{p}},z) v(\bar{\underset{\sim}{p}} - \underset{\sim}{p}') \,, \tag{32}$$

where

$$\Lambda(\underset{\sim}{P},\underset{\sim}{p},z) = \int \frac{d\omega}{2\pi} \frac{d\omega'}{2\pi} \frac{A(\frac{\underset{\sim}{P}}{2} + \underset{\sim}{p},\omega)\, A(\frac{\underset{\sim}{P}}{2} - \underset{\sim}{p},\omega')}{z - \omega - \omega'} [1 - f(\omega) - f(\omega')] \tag{33}$$

and $\underset{\sim}{P}$ is the center-of-mass momentum.

$T(z)$ is analytic in the upper and lower halves of the complex z plane, and

$$T^*(z) = T(z^*) .$$

Watson[21] has shown that if $v(r)$ is finite everywhere, $T(z)$ is bounded by a constant as $z \to \infty$. After performing the time integrations in (31)--by means of the δ functions--and transforming with respect to the coordinate variables, one can use the analytic properties of $G(z)$ and $T(z)$ to determine the Fourier coefficients of the self-energy, $\Sigma(z_\nu)$. Analytically continuing these coefficients, one has[5,9]

$$\Sigma(p,z) = \int \frac{d\underset{\sim}{p}'}{(2\pi)^3} \int \frac{d\omega}{2\pi} \Bigg[A(\underset{\sim}{p},\omega) f(\omega) \times \left\langle \frac{\underset{\sim}{p} - \underset{\sim}{p}'}{2} \left| T(\underset{\sim}{p} + \underset{\sim}{p}', \omega + z) \right| \frac{\underset{\sim}{p} - \underset{\sim}{p}'}{2} \right\rangle - G(\underset{\sim}{p}', \omega - z) f_b(\omega) \times \left\langle \frac{\underset{\sim}{p} - \underset{\sim}{p}'}{2} \left| T(\underset{\sim}{p} + \underset{\sim}{p}', \omega + i\epsilon) - T(\underset{\sim}{p} + \underset{\sim}{p}', \omega - i\epsilon) \right| \frac{\underset{\sim}{p} - \underset{\sim}{p}'}{2} \right\rangle \Bigg] - [\text{exchange terms}] , \qquad (34)$$

where

$$f_b(\omega) = [e^{\beta\omega} - 1]^{-1}$$

is the boson statistical factor. For a homogeneous, isotropic, unbounded system $A(\underset{\sim}{p},\omega)$ depends only on the magnitude of the momentum, $p = |\underset{\sim}{p}|$, and furthermore $\Sigma(\underset{\sim}{p}, z)$ does not depend on the orientation of $\underset{\sim}{p}$.

Equations (25), (32), and (34) are, explicitly, the set of coupled integral equations which must be solved in the TCTM approximation.

The theory could have been developed for a nonlocal potential by using a potential[9] of the form $\langle \underset{\sim}{r}_1 - \underset{\sim}{r}_2 | v | \underset{\sim}{r}_3 - \underset{\sim}{r}_4 \rangle$, corresponding to the local potential $\delta(|\underset{\sim}{r}_1 - \underset{\sim}{r}_2| - |\underset{\sim}{r}_3 - \underset{\sim}{r}_4|) \, v(|\underset{\sim}{r}_1 - \underset{\sim}{r}_2|)$. If one had carried out the development for this potential, the $v(\underset{\sim}{p} - \underset{\sim}{p}')$ in T would be replaced by $\langle \underset{\sim}{p} | v | \underset{\sim}{p}' \rangle$; we assume that the potential in (32) has this form.

Because of the complexity of this set of equations we must make a further approximation to facilitate their solution. We wish to make a partial-wave expansion of T , hence we perform a Brueckner-Gammel[3,5] type of averaging rather than actually performing the angular integrations in (32). This means we set

$$\left| \frac{\underset{\sim}{P}}{2} \pm \underset{\sim}{p} \right| \rightarrow p^{\pm} = \left(p^2 + \frac{P^2}{4} \pm \frac{pP}{\sqrt{3}} \right)^{1/2} \qquad (35)$$

in $\Lambda(\underset{\sim}{P}, \underset{\sim}{p}, z)$, which decouples the partial waves. This approximation can cause our solution to violate Baym's criterion, but we hope this violation is minor enough so that it does not affect the thermodynamic results. (A point to be confirmed at the completion of the calculation.)

A partial-wave expansion of T and v is made, and the partial-wave components, T_ℓ , of T are given by

$$\langle p|T_\ell(P,z)|p'\rangle = \langle p|v_\ell|p'\rangle + \int \frac{\bar{p}^2 d\bar{p}}{(2\pi)^3} \int \frac{d\omega}{2\pi} \frac{d\omega'}{2\pi}$$

$$\times \langle p|T_\ell(P,z)|\bar{p}\rangle \frac{A(\bar{p}^+,\omega)A(\bar{p}^-,\omega')[1 - f(\omega) - f(\omega')]}{z - \omega - \omega'} \langle \bar{p}|v_\ell|p'\rangle . \tag{36}$$

For liquid He^3 we need to consider a system of particles with spin $\frac{1}{2}$, interacting via a spin-independent interaction. The only complication introduced by spin is that the momentum and coordinate integrations contain an implicit sum over spin states. The direct part of Σ is multiplied by 2 as a result of this summation, and, since we have no spin-flip mechanism in our interaction, the exchange part is unaffected. Making the partial-wave expansion and using the summation relation for the spherical harmonics, we have, for the direct and exchange contributions to Σ,

$$2\langle \underset{\sim}{p}|T(\underset{\sim}{P},z)|\underset{\sim}{p}'\rangle - \langle \underset{\sim}{p}|T(\underset{\sim}{P},z)|-\underset{\sim}{p}'\rangle$$

$$= \sum_{\ell=0}^{\infty} \frac{2\ell + 1}{4\pi} [2 - (-1)^\ell] \langle p|T_\ell(P,z)|p'\rangle .$$

The spin sum contributes a factor of 2 to the expression for $\langle \frac{N}{\mathcal{V}} \rangle$ and $\langle \frac{\mathcal{H}}{\mathcal{V}} \rangle$ [Eqs. (19) and (20)]. One can perform the angular integrations in the expressions for these quantities to obtain, finally,

$$\left\langle \frac{N}{\mathcal{V}} \right\rangle^{\mu,\beta} = \int_{-\infty}^{\infty} \frac{d\omega}{2\pi} \int_0^{\infty} \frac{p^2 dp}{\pi^2} A(p,\omega) f(\omega) \tag{37}$$

and

$$\left\langle \frac{\mathcal{H}}{\mathcal{V}} \right\rangle^{\mu,\beta} = \int_{-\infty}^{\infty} \frac{d\omega}{2\pi} \int_{0}^{\infty} \frac{p^2 dp}{2\pi^2} \left(\omega + \frac{p^2}{2m} - \mu\right) A(p,\omega)\, f(\omega) \,. \tag{38}$$

Part B. The $\langle T \rangle_0$ Approximation with a Separable Potential (Zero Temperature)

The remainder of this paper is devoted to a zero-temperature calculation of the properties of liquid He^3 in an approximation to the TCTM approximation of Part A. This approximation, which we call the $\langle T \rangle_0$ approximation, retains the essential features of the TCTM approximation and should be considered as a first step toward the complete calculation.

We have also chosen to use a separable potential to describe the interaction of two free helium atoms. This results in a closed expression for the interaction of two atoms in the medium, with consequent simplification of the calculation.

The calculation was performed on the Lawrence Radiation Laboratory's IBM 7094 computer and the University of California at San Diego's CDC 3600 computer.

IV. TWO-BODY INTERACTION IN THE MEDIUM

We obtain the $\langle T\rangle_0$ approximation by replacing the spectral function in the equation for $\langle T\rangle$, (33), by

$$A_0(p,\omega) = 2\pi\,\delta\left(\omega - \frac{p^2 - p_f^2}{2m}\right).$$

Our approximation now is no longer thermodynamically consistent. The ω integrations in the equation for $\langle T\rangle$ are trivial, and we have the equation for $\langle T\rangle$ in the $\langle T\rangle_0$ approximation

$$\langle \underset{\sim}{p} \,|T(\underset{\sim}{P},z)|\, \underset{\sim}{p}'\rangle_0 = \langle \underset{\sim}{p} \,|v|\, \underset{\sim}{p}'\rangle + \int \frac{d\bar{\underset{\sim}{p}}}{(2\pi)^3} \frac{\langle \underset{\sim}{p} \,|T(\underset{\sim}{P},z)|\, \bar{\underset{\sim}{p}}\rangle_0 \, S(\bar{p}^+,\bar{p}^-)\langle \bar{\underset{\sim}{p}} \,|v|\, \underset{\sim}{p}'\rangle}{z - \frac{p^2}{m} + \frac{p_f^2}{m} - \frac{P^2}{4m}}, \tag{39}$$

where

$$S(p^+,p^-) = 1 - f\left(\frac{p^{+2} - p_f^2}{2m}\right) - f\left(\frac{p^{-2} - p_f}{2m}\right).$$

In the zero-temperature limit,

$$S(p^+,p^-) = \begin{cases} -1 & \text{for} \quad p^+,p^- < p_f \quad \text{(hole-hole)}, \\ 0 & \text{for} \quad p^- < p_f < p^+ \quad \text{(particle-hole)}, \\ 1 & \text{for} \quad p^+,p^- > p_f \quad \text{(particle-particle)}. \end{cases} \tag{40}$$

This approximation for $\langle T \rangle$ retains the essential features of the fermion system (it involves no approximations with regards to statistics) in contrast with the approximations which have been used to date. The Brueckner-Gammel[3] calculation neglects the hole-hole term; the calculations of Mills[5] and Puff-Martin[9] are formulated so that they have none of the features present in (40) (this is discussed in more detail in Section VI); Sung[4] makes a correction for the statistics, but his correction is a very poor approximation to the result obtained by solving with the statistical factors included.

It is well known[22] that v_ℓ can always be expressed in a separable form:

$$\langle p \,|v_\ell|\, p' \rangle = \frac{1}{m} \sum_{i=1}^{\infty} \lambda_\ell^{(i)} \, v_\ell^{(i)}(p) \, v_\ell^{(i)}(p') \, .$$

We assume that we can represent v_ℓ by only a few terms of the series. For $\ell = 0, 1, 2, 3$ we retain two terms of the series, for $\ell = 4, 5, 6$ only the first term; $T_\ell(P,z)$ is negligible for larger ℓ. This particular approximation does not affect Baym's criterion for thermodynamic consistency, but the $\langle T_\ell \rangle$ we obtain may not represent the liquid He^3 system accurately. We have of course lost self-consistency by our first approximation--as incorporated in (39).

We choose a form for the $v_\ell^{(i)}$'s and solve the scattering matrix for two free He^3 atoms. The coupling constants and parameters in our potentials are adjusted to match the phase shift calculated from potentials in coordinate space for He^3. The coordinate space

potentials are local potentials whose parameters are adjusted by means of the virial expansion to fit the experimental data for gaseous He^3.[6,7] The forms we choose for our separable potential and the determination of the parameters are discussed in Appendix A.

The separable potential allows us to write $\langle T_\ell \rangle_0$ in closed form:

$$\langle p \,|T_\ell(P,z)|\, p' \rangle_0 =$$

$$= \frac{(2\pi)^3}{m} \left[\begin{pmatrix} v_\ell^{(1)}(p) \\ v_\ell^{(2)}(p) \end{pmatrix} M_\ell(P,z) \begin{pmatrix} v_\ell^{(1)}(p') \\ v_\ell^{(2)}(p') \end{pmatrix} \right] [\det M_\ell(P,z)]^{-1} , \tag{41}$$

where

$$M_\ell(P,z) = \begin{bmatrix} g_\ell^{\,2} - I_\ell^{\,22}(P,z) & I_\ell^{\,12}(P,z) \\ I_\ell^{\,12}(P,z) & g_\ell^{\,1} - I_\ell^{\,11}(P,z) \end{bmatrix} ,$$

$$g_\ell^{\,i} = \frac{(2\pi)^3}{\lambda_\ell^{(i)}}$$

and

$$I_\ell^{\,ij}(P,z) = \frac{1}{m} \int_0^\infty p^2 \, dp \, \frac{v_\ell^{(i)}(p)\, v_\ell^{(j)}(p)\, S(p^+,p^-)}{z - \frac{p^2}{m} + \frac{p_f^{\,2}}{m} - \frac{P^2}{4m}} . \tag{42}$$

We need $\langle T_\ell(z)\rangle_0$ only for $z = \omega + i\epsilon$ and define the integrals (42) by introducing a physical cut from $\omega_0 = \frac{p^2}{4m} - \frac{p_f^2}{m}$ to $+\infty$.

If p_0 is defined by

$$\frac{p_0^2}{m} = \omega - \frac{p^2}{4m} + \frac{p_f^2}{m} \tag{43}$$

and the $I_\ell(\omega + i\epsilon)$'s examined for $p_0^2 < 0$, we see that the I_ℓ's are real, and consequently $\langle T\rangle_0$ is real. We have in this case

$$I_\ell^{ij}(P,\omega + i\epsilon) = \int_0^{p_1} p^2\,dp\,\frac{v_\ell^{(i)}(p)\,v_\ell^{(j)}(p)}{|p_0|^2 + p^2} - \int_{p_2}^{\infty} p^2\,dp\,\frac{v_\ell^{(i)}(p)\,v_\ell^{(j)}(p)}{|p_0|^2 + p^2}, \tag{44}$$

where p_1 and p_2 are solutions of

$$p^+(P,p_1) = p_f$$

and

$$p^-(P,p_2) = p_f .$$

If we had a potential which consisted of a single repulsive term, then (41) would become

$$\langle p\,|T_\ell(P,z)|\,p'\rangle = \frac{(2\pi)^3}{m}\,\frac{v_\ell^{(1)}(p)\,v_\ell^{(1)}(p')}{\left[g_\ell^{\,1} - I_\ell^{\,11}(P,z)\right]}, \tag{45}$$

where $g_\ell^{\,1}$ is positive; for I_ℓ given by (44) it would be possible for the denominator of (45) to be zero, and hence we would get a pole in $\langle T\rangle_0$. For the potentials we employ and when $\ell = 0$, we get this type of pole in $\langle T\rangle_0$ when $P < p_f$ and when $p_0^{\,2}$ is negative and very small (e.g., Figs. 2 and 3, where the small imaginary part at the pole in Fig. 3 is due to the angular integration which has been performed). We know that $\Gamma(p,\omega)$ should not be zero in this region, and if it is nonzero the imaginary part of $\langle T\rangle$ will not be zero in this region, and hence we would not have a pole. The integration of the real part of $\langle T\rangle_0$ through the pole will behave like a principal-value integral, and consequently we have simply removed the singularity by smoothing the real part of $\langle T\rangle_0$, as depicted by the dotted lines for negative ω in Fig. 2.

For $p_0^{\,2} \gg 0$ the form of our potentials is such that if we neglect $g_\ell^{\,1}$ we obtain

$$\langle p\,|T_\ell(P,\,\omega + i\epsilon)|\,p\rangle \;\sim\; -[v_\ell^{(1)}(p)]^2\, p_0[\tan(p_0 r_c - \tfrac{\pi}{2}(\ell+1)) + i]\,,$$

which clearly has the property that the real part of $\langle T\rangle_0$ is highly singular for large p_0. Our numerical procedures do not adequately handle these singularities and we have had to smooth $\langle T\rangle_0$ for large values of p_0. The procedure we employ is motivated by the following reasoning: The angular integrations

$$\int_{-1}^{1} d(\cos\theta_{p'})\,\langle\,\left|\frac{\underset{\sim}{p}-\underset{\sim}{p}'}{2}\right|\,\left|T_\ell\left(\left|\frac{\underset{\sim}{p}+\underset{\sim}{p}'}{2}\right|,\,\omega+i\epsilon\right)\right|\,\left|\frac{\underset{\sim}{p}-\underset{\sim}{p}'}{2}\right|\,\rangle$$

must be performed, or, considering only the real part,

$$- \int d(\cos \theta_{p'})\, r_c\, p_0 \left[\tan\left(p_0\, r_c - \frac{\pi}{2}(\ell + 1)\right)\right]\left[v_\ell^{(1)}\left(\frac{|\underset{\sim}{p} - \underset{\sim}{p}'|}{2}\right)\right]^2 ,$$

where

$$p_0^{\,2} = \omega - \frac{p^2 + p'^2}{4} - \frac{pp' \cos \theta_{p'}}{2} + p_f^{\,2} .$$

Changing variables--and ignoring constants--we obtain terms like

$$M_\ell = -2 \int ds\, s^2 \tan\left[s - \frac{\ell + 1}{2}\pi\right] ,$$

where $s = p_0 r_c$. For ℓ odd we integrate from $n\pi - \pi/2$ to $n\pi + \pi/2$, and for ℓ even from $n\pi$ to $(n + 1)\pi$. Consequently

$$M_\ell = 4n\pi^2[0.693] \qquad \text{for} \quad \ell \text{ odd} ,$$

$$M_\ell = 4(n + \tfrac{1}{2})\pi^2\,[0.693] \quad \text{for} \quad \ell \text{ even},$$

or

$$M_\ell(n\pi) = 4n\pi^2[0.693] ;$$

hence we make the replacement

$$r_c p_0 \tan\left[p_0 r_c - \frac{\pi}{2}(\ell + 1)\right] \rightarrow 1.386$$

when p_0 is large. The effect of this smoothing is discussed, along with the numerical results, in Section IV.

The separable potentials, fitted to the de Boer[7] phase-shift data (see Appendix A), are numerically integrated by using a Gaussian quadrature formula[23] to obtain the I_ℓ^{ij} integrals. The angular integration in (34) is independent of both G and A, so we find it useful to evaluate

$$R(p,p',\omega + i\epsilon) = 2\pi \int_{-1}^{1} d(\cos\theta_{p'}) \sum_{\ell=0}^{6} (2 - (-1))^{\ell}$$

$$\times \frac{(2\ell + 1)}{4\pi} \left\langle \left| \frac{\underset{\sim}{p} - \underset{\sim}{p}'}{2} \right| \left| T_\ell \left(\left| \underset{\sim}{p} + \underset{\sim}{p}' \right|, \omega + i\epsilon \right) \right| \left| \frac{\underset{\sim}{p} - \underset{\sim}{p}'}{2} \right| \right\rangle_0 , \tag{46}$$

which is symmetric in p and p'. R is the complex two-body interaction, defined so that

$$R(p,p',\omega + i\epsilon) = \text{Re } R(p,p',\omega) - i \text{ Im } R(p, p', \omega)$$

which is used to compute $\Sigma(p,\omega)$. In Figs. 2 and 3 we have plotted the real and imaginary parts of R, respectively, for a typical value of p_f and several values of p.

V. THE SPECTRAL FUNCTION (SELF-ENERGY)

Inserting this complex two-body interaction (46), into (34) and writing

$$G(p, \omega + i\epsilon) = \frac{1}{2}\,[B(p,\omega) - i\,A(p,\omega)]$$

and

$$\Sigma(p, \omega + i\epsilon) = \text{Re}\,\Sigma(p,\omega) - \frac{i}{2}\,\Gamma(p,\omega)\ ,$$

we obtain

$$\text{Re}\,\Sigma(p,\omega) = \int_0^\infty \frac{p'^2 dp'}{(2\pi)^3} \int_{-\infty}^{0} \frac{d\omega}{2\pi}\,[A(p',\omega')\ \text{Re}\,R(p,p',\omega' + \omega) + B(p',\omega' - \omega)\ \text{Im}\,R(p,p',\omega')] \tag{47a}$$

and

$$\Gamma(p,\omega) = 2\int_0^\infty \frac{p'^2 dp'}{(2\pi)^3} \int_{-\omega}^{0} \frac{d\omega'}{2\pi}\,A(p',\omega')\ \text{Im}\,R(p,p',\omega' + \omega)\ , \tag{47b}$$

where the zero-temperature forms of $f(\omega')$ and $f_b(\omega')$ have been used to define the limits for the ω' integrations. These equations, and (24):

$$G(p, \omega + i\epsilon) = [\omega - \epsilon(p,\omega) + \frac{i}{2}\,\Gamma(p,\omega)]^{-1} \tag{48}$$

where

$$\epsilon(p,\omega) = \frac{p^2}{2m} - \mu + \text{Re}\,\Sigma(p,\omega)\ , \tag{49}$$

form the set of equations which we need to solve self-consistently.

The spectral function $A(p,\omega)$, Eq. (25), is sharply peaked at the single-particle energy, which we define as the solution of

$$\epsilon(p) - \epsilon(p, \epsilon(p)) = 0 ; \tag{50}$$

the ω integrations involving $A(p,\omega)$ in the interval

$$d = [\epsilon(p) - |0.075\epsilon(p)|, \epsilon(p) + |0.075\epsilon(p)|]$$

are performed by replacing $A(p,\omega)$ by a δ function,

$$A(p,\omega) = w(p)\, \delta(\omega - \epsilon(p)) ,$$

in this interval. $A(p,\omega)$ is well behaved outside the interval d, and the integrations outside this interval are performed by Gaussian quadrature. The sum rule, (18), can be employed to determine $w(p)$:

$$w(p) = 1 - \left[\int_{-\infty}^{\epsilon(p)-\frac{d}{2}} + \int_{\epsilon(p)+\frac{d}{2}}^{\infty} \right] \frac{d\omega}{2\pi} A(p,\omega) . \tag{51}$$

The integration of $B(p,\omega)$ over the interval d is obtained by letting

$$B(p,\omega) = 2 \frac{\rho(p)[\omega - \epsilon(p)]}{[\omega - \epsilon(p)]^2 + [\gamma(p)]^2}$$

and expanding the imaginary part of R in a Taylor's series about $\omega = \epsilon(p)$. Retaining only the first two terms in this expansion, we have

$$\int_d d\omega' \; B(p',\omega') \; \mathrm{Im}\, R(p,p',\omega+\omega')$$

$$= 4\rho(p') \left.\frac{\partial \; \mathrm{Im}\, R(p,p',\omega')}{\partial \omega'}\right|_{\omega'=\omega+\epsilon(p')}$$

$$\times \left[0.075\;|\epsilon(p')| \; - \gamma(p') \tan^{-1} \frac{0.075|\epsilon(p')|}{\gamma(p')}\right] .$$

The Fermi momentum, p_f, is defined as the solution of

$$\frac{p_f^2}{2m} - \mu + \mathrm{Re}\,\Sigma(p_f,0) = \epsilon(p_f,0) = 0 . \tag{53}$$

However, the behavior of the statistical factors and the form of the interaction make it easier to carry out the calculation for a fixed p_f and use (53) to determine μ.

The calculation thus proceeds as follows: for a given p_f we calculate $R(p,p',\omega+i\epsilon)$, (46); we then choose a trial solution $G_t(p,\omega+i\epsilon)$ for (48) and use this trial solution in (47) to generate a new trial solution. This process is repeated until the trial solution reproduces itself; when the solution has converged we use the resulting spectral function, (25), in (37) and (38) to calculate $\langle N/\mathcal{V}\rangle$ and $\langle \mathcal{H}/\mathcal{V}\rangle$.

The convergence of this procedure is rapid, as may be seen in Fig. 4, where $\epsilon(p)$ is plotted for a number of iterations in which

the initial choice of a spectral function was

$$A_0(p,\omega) = 2\pi\, \delta\left(\omega - \frac{p^2 - p_f^2}{2m}\right) .$$

For $p \gg p_f$ the convergence is even more rapid, since the single-particle energy is dominated by the kinetic term.

In Fig. 5 we have plotted $\epsilon(p,\omega)$, (49), for a typical value of p_f and some values of p near p_f. We have also drawn the line $\epsilon = \omega$ whose intersection with $\epsilon(p,\omega)$ gives $\epsilon(p)$, (50). In Fig. 6 we have plotted the values of $\epsilon(p)$ versus p for the same value of p_f. One sees that because of the behavior of $\epsilon(p,\omega)$, when ω is near zero and p is in the neighborhood of p_f, there is a sharp break in $\epsilon(p)$ near p_f. Since there is only a single intersection of the line $\epsilon = \omega$ with $\epsilon(p,\omega)$, there is no gap in $\epsilon(p)$ and we have a "normal" fermion system.

The peculiar behavior of $\epsilon(p,\omega)$ near the Fermi surface comes about owing to the presence of the second integral on the right-hand side of Eq. (47a). This integral involves Im $R(\omega)$ for $\omega < 0$, which is precisely the region where we have the least confidence in our interaction because of the presence of the pole--which is treated only approximately. Also, there is essentially a principal-value integral which has to be evaluated when p is near p_f, with consequent difficulty in obtaining reliable results from the numerical evaluations. This integral was evaluated in a number of ways to determine if this behavior was due to the numerical methods used; we found

that the behavior was real and not a result of the numerical integration. The approximations involved in obtaining the interaction preclude any prediction that this behavior is a characteristic of the real physical system, and possibly it will not be present in the TCTM approximation discussed in Part A of this paper. Indeed, we see in Fig. 7, where we have plotted $\epsilon(p,\omega)$ for a larger range of ω and p values--and not amplified the region near $\omega = 0$ --that $\epsilon(p,\omega)$ is a reasonably well-behaved function of ω and p .

If one examines the behavior of $\langle T \rangle_0$ near the pole (see Fig. 2), it has the form

$$\langle\, T(\omega + i\epsilon)\,\rangle_0 \approx \frac{s}{\omega + \omega_0 + i\epsilon} + t(\omega) ,$$

where ω_0 and s are negative and $t(\omega)$ is a smooth function. Consequently, inclusion of the pole would give an additional negative contribution to $\mathrm{Im}\, R(\omega)$ for $\omega < 0$. However, most of the contribution to $\epsilon(p,\omega)$ from $\mathrm{Im}\, R$ is proportional to $\partial\, \mathrm{Im}\, R/\partial\omega$, (52), and this analysis gives no information concerning the resulting effect on $\epsilon(p,\omega)$.

For p_f less than $0.80\ \mathring{A}^{-1}$ the intersection of the line $\epsilon = \omega$ with $\epsilon(p,\omega)$ occurs in a region where $\epsilon(p,\omega)$ has a positive slope (e.g., Fig. 4) for momentum points near p_f . When this happens the iteration procedure becomes unstable and we are not able to obtain a solution to the equations.

In Fig. 8 we plot $\Gamma(p,\omega)$ for the same value of p_f as employed in the above mentioned graphs. Luttinger[20] has proven that to arbitrary order in perturbation theory, at zero temperature,

$$\Gamma(\omega) \xrightarrow[\omega \to 0]{} c\,\omega^2 ,$$

where c is a positive constant. It can be seen that the solution satisfies this criterion. The behavior of $\Gamma(p,\omega)$ for $\omega > 0$ is determined by the behavior of $\mathrm{Im}\,\langle T(\omega)\rangle_0$ for $\omega > 0$. For small relative momentum, and $\omega > 0$, $\mathrm{Im}\,\langle T(\omega)\rangle_0$ is dominated by the hard shell. Consequently, for $p < p_f$, and $\omega > 0$, this aspect of the two-body potential dominates the behavior of $\Gamma(p,\omega)$.

This effect of the hard shell is clearly seen in the momentum-density distribution function,

$$n(p) = \int_{-\infty}^{0} \frac{d\omega}{2\pi}\, A(p,\omega) , \qquad (54)$$

which is plotted in Fig. 9. For an ideal Fermi gas the momentum density is unity for $p < p_f$ and zero for $p > p_f$; for this calculation $n(p) < 1$ for $p < p_f$, since $\Gamma(p,\omega) > 0$ for $\omega > 0$.

In Section IV it was asserted that a pole in $\langle T\rangle$ would not be present if a more reasonable $A(p,\omega)$ were employed than the one used to obtain $\langle T\rangle_0$. In Fig. 8a one can see that $\Gamma(p,\omega)$ has a value comparable to $\epsilon(p)$ for small values of p and $\omega < 0$, and from the analysis above and Eq. (47b) one sees that the inclusion of the pole in the interaction would make $\Gamma(p,\omega)$ larger for $\omega < 0$. A step

toward obtaining the TCTM approximation would be to use the output spectral function in $\langle T \rangle$ to obtain a new interaction, and in that approximation $\langle T \rangle$ would be a smooth function for $\omega < 0$. A larger $\Gamma(p,\omega)$ would tend to further smooth $\langle T \rangle$; hence the approximation of eliminating the pole is reasonable.

The error that results from the smoothing of $\mathrm{Re}\langle T \rangle_0$ for large values of p_0 , (48), reflects in the behavior of $\epsilon(p,\omega)$ for values of $\omega \gg \epsilon(p)$. Since $A(p,\omega)$ is sharply peaked near $\epsilon(p)$, an error in this region should not affect its shape, but such an error can clearly alter the value of $w(p)$, (51). Because $A(p,\omega)$ is such a peaked function it is not very instructive to plot it; we have thus plotted $w(p)$, which is a measure of the amount of $A(p,\omega)$ contained in the peak in Fig. 10.

VI. THERMODYNAMIC QUANTITIES AND COMPARISON WITH OTHER THEORIES

The spectral functions calculated in the $\langle T \rangle_0$ approximation and the two-body interaction cannot be expected to give accurate quantitative agreement with the experimentally determined thermodynamic properties of liquid He^3. However, the spectral functions have a reasonable form, and so we are stimulated to go ahead and evaluate the thermodynamic properties, which we then compare both with experiment and with other calculations.

The experimental curves in the figures are obtained by extrapolating the P-V-T data of Sherman and Edeskuty[24] to zero degrees and integrating to obtain $\langle E/N \rangle$. We determine μ by substituting (10) into (12).

The ground-state properties, for various calculations now to be discussed, are compared with the experimental values in Table I.

1. Mills Approximation

Mills[5] has used separable potentials very similar to those in Appendix A, fitted to the de Boer data, and a simple extension of the Hartree-Fock approximation[15] which consists of replacing the potential by the two-body scattering matrix,

$$\langle \underset{\sim}{p} \mid S(\Omega) \mid \underset{\sim}{p}' \rangle = \langle \underset{\sim}{p} \mid v \mid \underset{\sim}{p}' \rangle + \mathcal{P} \int \frac{d\bar{\underset{\sim}{p}}}{(2\pi)^3} \frac{\langle \underset{\sim}{p} \mid S(\Omega) \mid \bar{\underset{\sim}{p}} \rangle \langle \bar{\underset{\sim}{p}} \mid v \mid \underset{\sim}{p}' \rangle}{\Omega - \bar{p}^2} ,$$

where $\Omega = (p^2/4) + p^2 - 2\mu$, and he has used the stationary boundary condition to obtain a real S. For the self-energy, he has

$$\Sigma(p, \frac{p^2}{2} - \mu) = \int \frac{dp'}{(2\pi)^3} \int \frac{d\omega}{2\pi} A(p',\omega) f(\omega)$$

$$\times \left[\left\langle \frac{p - p'}{2} \left| S\left(\frac{p^2 + p'^2}{2} - 2\mu \right) \right| \frac{p - p'}{2} \right\rangle - \left| \frac{p' - p}{2} \right\rangle \right] ,$$

with

$$A(p,\omega) = 2\pi \, \delta(\omega - \epsilon(p))$$

and

$$\epsilon(p) = \frac{p^2}{2m} - \mu + \Sigma(p, \frac{p^2}{2} - \mu) .$$

Baym[11] has shown that the Hartree-Fock approximation is a thermodynamically consistent approximation (see Fig. 1) and Mills's results satisfy the Hugenholtz-Van Hove theorem, (11). However, Mills has described a physically unrealizable system with negative pressure.

2. Sung's Approximation

Another calculation of ground-state properties, starting from a two-body interaction, was performed by Sung.[4] He calculated the phase shift from Schrödinger's equation for the Yntema-Schneider and 6-12 potentials with an effective mass, m^*, and replaced $\langle T \rangle$ in Σ by the real part of the free-particle scattering matrix,

$$\langle p \left| S_\ell\left(\frac{p^2}{2m^*} + i\epsilon \right) \right| p \rangle = - \frac{(4\pi)^2}{m^* p} \sin \delta_\ell(p) \, e^{i\delta_\ell(p)} ,$$

less a term to partially account for the statistical factors; also A is taken to be

$$A(p,\omega) = 2\pi\,\delta\left(\omega - \frac{p^2 - p_f^2}{2m^*}\right) .$$

The effective mass is adjusted until the output value

$$\frac{1}{m^*} = \lim_{p \to p_f} \frac{\partial\Sigma(p)}{\partial(p^2)}$$

is the same as the input value, and this value of m^* is used to calculate the ground-state energy. He performed calculations only for $p_f^3/3\pi^2$ equal to the experimental density, and made no attempt to find the minimum in the energy-versus-density curve.

3. Puff-Martin Approximation

Figure 11 shows $\langle E/N \rangle$ and μ versus density, for liquid He^3, calculated using the Puff-Martin approximation.[9] This calculation was performed[1] with the potentials in Appendix A. It involves using

$$G_0(p,z) = \left[z - \frac{p^2}{2m} + \mu\right]^{-1}$$

with $\mu < 0$ in the T matrix, (32). The resulting

$$\langle \underset{\sim}{p} \,|T(\underset{\sim}{P},z)|\, \underset{\sim}{p}' \rangle_{PM} = \langle \underset{\sim}{p} \,|v|\, \underset{\sim}{p}' \rangle + \int \frac{d\bar{\underset{\sim}{p}}}{(2\pi)^3} \frac{\langle \underset{\sim}{p} \,|T(\underset{\sim}{P},z)|\, \bar{\underset{\sim}{p}} \rangle_{PM} \langle \bar{\underset{\sim}{p}} \,|v|\, \underset{\sim}{p}' \rangle}{z - \frac{P^2}{4m} - \frac{\bar{p}^2}{m} + 2\mu}$$

is real for $z \to \omega + i\epsilon$, where $\omega < 0$. From Eqs. (47) one sees that

$\Sigma(p,\omega)$ is real for $\omega < 0$, and, examining (50) and (53), one sees that for $p < p_f$ and $\omega < 0$ the spectral function, (25), is

$$A(p,\omega) = 2\pi\, \rho(p)\, \delta(\omega - \epsilon(p)) ,$$

where

$$\rho(p) = \left[1 - \frac{\partial \epsilon(p,\omega)}{\partial \omega}\bigg|_{\omega=\epsilon(p)} \right]^{-1} .$$

Using this spectral function in (37) and (38), one sees clearly that only $\epsilon(p)$ is needed for $p < p_f$; hence one need only solve

$$\epsilon(p) = \frac{p^2}{2m} - \mu + \text{Re}\ \Sigma(p,\epsilon(p))$$

and

$$\text{Re}\ \Sigma(p,\omega) = \int_0^{p_f} \frac{d\underset{\sim}{p}'}{(2\pi)^3}\ \rho(p')$$

$$\times \left[\left\langle \frac{\underset{\sim}{p} - \underset{\sim}{p}'}{2} \left| T(\omega + \epsilon(p') + i\epsilon) \right| \frac{\underset{\sim}{p} - \underset{\sim}{p}'}{2} \right\rangle - \left| \frac{\underset{\sim}{p}' - \underset{\sim}{p}}{2} \right\rangle \right]$$

and the expression for $\rho(p)$ self-consistently for $\epsilon(p) < 0$. In the nuclear-matter calculation, Puff[9] determined the ground-state Fermi momentum, p_f , by the criterion that the Hugenholtz-Van Hove theorem, (11), was satisfied. Falk and Wilet[25] pointed out that Puff's ground-state solution did not have zero pressure as determined by Eq. (10); they used this last criterion to determine the ground-state solution.

The curve for this approximation in Fig. 11 was obtained by using the potential fitted to the de Boer data. The potentials with these parameters just managed to produce a solution which satisfies

$$\frac{\partial}{\partial\left(\frac{N}{V}\right)}\left(\frac{E}{N}\right) = 0 , \qquad (55)$$

but was not able to produce a solution that satisfies (11) with the constraint $\mu \leq 0$. The calculation was also performed with the potential parameters adjusted to reproduce the phase shift from the Yntema-Schneider potential; no solution was found in this case.

4. Brueckner-Gammel Approximation

The Brueckner-Gammel[3] calculation was not formulated by use of thermodynamic Green's functions; it is difficult to describe in these terms. The essential features are included if we take

$$A(p,\omega) = 2\pi\,\delta(\omega - \epsilon(p)) \qquad \text{for} \qquad p < p_f ,$$

and

$$A(p,\omega) = 2\pi\,\delta(\omega - \epsilon(p,\Omega)) \qquad \text{for} \qquad p > p_f ,$$

in $\langle T \rangle$, (32), and Σ, (34). Here Ω is to be determined from a supplementary condition. Brueckner and Gammel argue that the "hole-hole" term can be neglected and hence the integration in $\langle T \rangle$ for the momentum is restricted to p^+ and $p^- > p_f$. Also the interaction matrix is real for all $\epsilon(p,\Omega)$, since they calculate $\langle T \rangle$ off the "energy shell" for these values. Their results[26] do not satisfy the Hugenholtz-Van Hove theorem, as was pointed out in the original paper.[16]

5. $\langle T \rangle_0$ Approximation

The spectral functions, which are calculated for different p_f's, when used in Eq. (37) and (38) allow us to calculate $\langle N/\mathcal{V} \rangle^{\mu,\infty}$. Substituting (54) into (37) yields, for the density,

$$n = \left\langle \frac{N}{\mathcal{V}} \right\rangle^{\mu,\infty} = \int_0^\infty \frac{p^2\,dp}{\pi^2}\, n(p) \; ; \qquad (56)$$

using (5) and (38) yields, for the average energy per particle,

$$e = \left\langle \frac{E}{N} \right\rangle^{\mu,\infty} = \frac{1}{n} \int_0^\infty \frac{p^2\,dp}{\pi^2} \times \int_{-\infty}^0 \frac{d\omega}{2\pi}\, \frac{1}{2}\left(\omega + \frac{p^2}{2m} + \mu\right) A(p,\omega) \; . \qquad (57)$$

In Fig. 12 we display e and μ versus n. The results for μ are not as accurate as those for e, since μ is obtained using Eq. (53), which, as we see in Fig. 4, involves the intersection of two curves with comparable slope, while e is obtained by integration of Eq. (57). In Fig. 13 we plot n versus p_f, and for comparison we also plot $p_f^2/3\pi^2$, which is the density of an ideal Fermi gas corresponding to the momentum p_f. From Figs. 12 and 13 we see that the density at which (55) is satisfied corresponds to a Fermi momentum less than $0.80\ \text{Å}^{-1}$. As was explained in Section V, the iteration procedure becomes unstable for values of p_f below this value.

However, the minimum appears to be close to $p_f = 0.80\ \mathring{A}^{-1}$, and we have extrapolated the calculated values to determine the minimum.

One can see, in Fig. 12, that the Hugenholtz-Van Hove theorem, Eq. (11), is not satisfied for this approximation (as we would expect, since this is not a thermodynamically consistent approximation), but the discrepancy is smaller in this calculation than in the other theoretical studies[26] (except that of Mills). In Fig. 14 P is plotted versus n, from the experimental data and also from Eqs. (10) and (12). These two expressions give different values for the pressure because our approximation is not thermodynamically consistent.

In view of the behavior of the single-particle energy, for p near p_f, we cannot obtain a meaningful value of m^* from the $\langle T \rangle_0$ calculation.

The use of the single-particle energy in $\langle T \rangle$ is an important feature of the Brueckner-Gammel calculation and presumably would be a desirable improvement in the calculation reported here. We have not performed this improved calculation (which would involve extensive computational time), but have moved directly to the more extensive computation reported in paper II of this series (where only the approximations described in Part A are made).

ACKNOWLEDGMENTS

One of the authors (D. E. Beck) would like to thank Professor K. A. Brueckner for discussions concerning the applicability of the approximations used in Part B, and for his illuminating comments concerning the relevance of the effects discussed in the papers of Bethe and Pitaevskii (Ref. 10) in the liquid helium-three problem. He would also like to acknowledge extensive correspondence with Mr. R. Prabhu and Dr. R. E. Mills in regards to the separable potentials.

APPENDIX A: A SEPARABLE POTENTIAL FOR He^3

In Chapter IV we introduced separable potentials which were employed to evaluate the T_0 matrix; this appendix is devoted to explaining our choice of potentials, and the method employed to determine the potential parameters so that these potentials can be considered to approximate the He^3 two-body interaction.

The choice of functional form for the potentials is rather arbitrary. The primary criterion is convenience; namely, a form which allows a maximum amount of analytic computation. The parameters are adjusted so that the phase shift resulting from the potentials approximates the phase shifts computed using the Lennard-Jones 6-12 and the Yntema-Schneider potentials.

The Lennard-Jones potential is

$$v(r) = \epsilon_0 \left[\left(\frac{\sigma}{r}\right)^{12} - \left(\frac{\sigma}{r}\right)^{6} \right],$$

with

$$(\epsilon_0/\kappa) = 40.88^{\circ}\,\mathrm{K}, \quad \sigma = 2.56\,\text{Å};$$

r is in angstroms, and κ is Boltzman's constant. This potential was fitted by de Boer et al.[7] to the low-temperature virial coefficients. The Yntems-Schneider potential[6] is

$$v(r) = \epsilon_0 \left[1200\, e^{-r/0.212} - \frac{1.24}{r^6} - \frac{1.89}{r^8} \right],$$

with $(\epsilon_0/\kappa) = 7250^{\circ}\,\mathrm{K}$; it was fitted by these authors to the virial coefficients up to $1000^{\circ}\,\mathrm{K}$. The phase shifts were computed by de Boer

et al.[7] for the Lennard-Jones potential and by Sung[29,1] for the Yntema-Schneider potential.

Puff has developed the expression for the phase shift in terms of the two-body scattering matrix for a separable potential; we quote the relevant formulae here. The scattering matrix is given by

$$\langle \underset{\sim}{p} \,|S(\Omega)|\, \underset{\sim}{p'}\rangle = \langle \underset{\sim}{p} \,|v|\, \underset{\sim}{p'}\rangle + \int \frac{d\underset{\sim}{p}}{(2\pi)^3} \frac{\langle \underset{\sim}{p}|S(\Omega)|\bar{\underset{\sim}{p}}\rangle\langle \bar{\underset{\sim}{p}} \,|v|\, \underset{\sim}{p'}\rangle}{\Omega - \frac{\bar{p}^2}{m}} , \tag{A.1}$$

and is related to the scattering amplitude by

$$f(\underset{\sim}{p}) = -\frac{m}{4\pi} \langle \underset{\sim}{p} \,|S(\frac{p_0^2}{m} + i\epsilon)|\, \underset{\sim}{p_0}\rangle .$$

Using the well-known relation[30] connecting the scattering amplitude and the phase shift yields

$$\tan \delta_\ell = -\frac{pm}{8\pi^2} \frac{\langle p \,|S_\ell(\frac{p^2}{m} + i\epsilon)|\, p\rangle}{2 - \frac{ipm}{8\pi^2}\langle p \,|S_\ell(\frac{p^2}{m} + i\epsilon)|\, p\rangle} , \tag{A.2}$$

where $\langle S\rangle$ has been expanded in partial waves. Choosing the potential, $\langle v\rangle$, in (A.1) to be a sum of separable potentials,

$$\langle p \,|v_\ell|\, p'\rangle = \frac{1}{m} \sum_{i=1}^{2} \lambda_\ell^{(i)} v_\ell^{(i)}(p) v_\ell^{(i)}(p') ,$$

one obtains a closed form for $\langle S_\ell\rangle$ identical to Eq. (41) with $P = 0$, and the integrals I_ℓ^{ij} replaced by

$$J_\ell^{ij}(\Omega) = \int_0^\infty p^2\, dp\, \frac{v_\ell^{(i)}(p)\, v_\ell^{(j)}(p)}{m\Omega - p^2} . \qquad (A.3)$$

One needs to evaluate (A.2) for $\Omega = (p^2/m) + i\epsilon$; this value of Ω allows one to write (A.3), when the symbolic identity

$$\frac{1}{\omega \pm i\epsilon} = P\frac{1}{\omega} \mp i\pi\, \delta(\omega)$$

is employed, in the form

$$J^{ij}\left(\frac{p^2}{m} + i\epsilon\right) = P\int_0^\infty p'^2\, dp'\, \frac{v^{(i)}(p')\, v^{(j)}(p')}{p^2 - p'^2} - i\frac{\pi}{2}\, p\, v^{(i)}(p)\, v^{(j)}(p) \qquad (A.4)$$

$$= \bar{J}^{ij}\left(\frac{p^2}{m}\right) - i\frac{\pi}{2}\, p\, v^{(i)}(p)\, v^{(j)}(p) .$$

Substituting for $\langle S \rangle$ in (A.2), we have the explicit formula

$$\tan \delta_\ell(p) = -\frac{p\pi}{2}\left[\begin{pmatrix} v_\ell^{(1)}(p) \\ v_\ell^{(2)}(p) \end{pmatrix} M_\ell\left(\frac{p^2}{m}\right) \begin{pmatrix} v_\ell^{(1)}(p') \\ v_\ell^{(2)}(p') \end{pmatrix}\right][\det M_\ell]^{-1} , \qquad (A.5)$$

where

$$M_\ell\left(\frac{p^2}{m}\right) = \begin{bmatrix} g_\ell^{\,2} - \bar{J}_\ell^{\,22}\left(\frac{p^2}{m}\right) & \bar{J}_\ell^{\,12}\left(\frac{p^2}{m}\right) \\ \bar{J}_\ell^{\,12}\left(\frac{p^2}{m}\right) & g_\ell^{\,1} - \bar{J}_\ell^{\,11}\left(\frac{p^2}{m}\right) \end{bmatrix} ,$$

and

$$g_\ell^{\,i} = \frac{(2\pi)^3}{\lambda_\ell^{(i)}} \ .$$

The Lennard-Jones 6-12 and the Yntema-Schneider potentials are both strongly repulsive for small interparticle separations. To replicate this we choose a two-term potential for $\ell = 0, 1, 2, 3$, with one term giving the short-range repulsion and the other term giving the long-range attraction. For $\ell = 4, 5, 6$ we use only an attractive term, since the "angular momentum barrier" shields the short-range repulsion.

The repulsive part of the potential is taken to be a "hard shell,"

$$\langle r' | v_\ell | r \rangle = v_\ell^{(1)}(r)\, v_\ell^{(1)}(r') = \frac{\delta(r - r_c)}{4\pi r_c^2} \frac{\delta(r' - r_c)}{4\pi r_c^2} ,$$

which yields, after a spherical Hankel transform has been performed,[31]

$$v_\ell^{(1)}(p) = j_\ell(\rho) ,$$

where $\rho = pr_c$ and the j_ℓ's are spherical Bessel functions.[29] For $\ell = 0, 1, 2$ we use

$$v_\ell^{(2)}(r) = -\frac{\theta(r - r_c)}{4\pi r_c^3}\, i^\ell\, h_\ell^{(1)}(i\alpha r) ,$$

where $\theta(r)$ is the Heaviside unit function (defined as zero for negative argument and unity for positive argument), and $h_\ell^{(1)}$ is a

spherical Hankel function of the first kind.[30] Transforming this potential, one obtains

$$v_\ell^{(2)}(p) = \frac{i^\ell}{\rho^2 + \beta^2} \left[i\beta \, j_\ell(\rho) \, h_{\ell-1}^{(1)}(i\beta) - \rho h_\ell^{(1)}(i\beta) \, j_{\ell-1}(\rho) \right] ,$$

where $\beta = \alpha r_c$ and r_c are two parameters yet to be determined. For $\ell = 3$ we use

$$v_\ell^{(2)}(r) = \frac{\theta(r - r_c)}{4\pi \, r_c^3} \left(\frac{r_c}{r} \right)^{\ell+1} ,$$

whose transform is

$$v_\ell^{(2)}(p) = \frac{j_{\ell-1}(\rho)}{\rho} .$$

The attractive potentials employed for $\ell = 4, 5, 6$ have no simple coordinate space representation; in momentum space they are

$$v_\ell^{(2)}(p) = \frac{\rho^\ell}{[\rho^2 + \beta^2]^{(\ell+1)/2}} .$$

Evaluating the integrals J_ℓ, one obtains $\tan \delta_\ell$, and then adjusts the various parameters to reproduce the phase shifts computed from the 6-12 and Yntema-Schneider potentials. The parameters which give the best fit to the phase-shift data are tabulated in Table II. The phase shift for the 6-12 potential[7] was available for 20 equally spaced momentum values between 0.086 and 1.564 Å^{-1} and for the Yntema-Schneider potential[21,1] for 25 momentum values between 0.86 and 1.954 Å^{-1}.

The separable potentials were fitted to these values, and the deviation quoted in Table II was computed by using

$$(\mathrm{Dev})_\ell = \left[\frac{1}{N} \sum_{n=1}^{N} \left[(2\ell + 1)\left(\delta_\ell^{\mathrm{deB\ or\ Y\text{-}S}}(n) - \delta_\ell^{\mathrm{Sep}}(n) \right) \right]^2 \right]^{1/2}, \tag{A.6}$$

where $N = 20$ or 25. The coupling constants for the repulsive core are taken as large, but finite, numbers,

$$\lambda_\ell^{(1)} \approx -(10^4 - 10^5)\lambda_\ell^{(2)} .$$

FOOTNOTES AND REFERENCES

* Supported in part by the U. S. Atomic Energy Commission.

† Based in part on a Ph.D. thesis (Ref. 1).

1. D. E. Beck, A Quantum Statistical Calculation of the Properties of Liquid Helium-Three (Ph.D. Thesis), Lawrence Radiation Laboratory Report UCRL-11679, September 1964.
2. P. C. Martin and J. Schwinger, Phys. Rev. 115, 1342 (1959); this paper is referred to as MS.
3. K. A. Brueckner and J. L. Gammel, Phys. Rev. 109, 1040 (1958).
4. C. C. Sung, Some Properties of He^3 (Part II of Ph.D. Thesis), University of California, Berkeley, 1964.
5. R. E. Mills, An Application of the Theory of Many Fermion Systems to Liquid Helium-Three (Ph.D. Thesis), Ohio State University, 1963.
6. J. L. Yntema and W. G. Schneider, J. Chem. Phys. 18, 641 (1950).
7. J. de Boer, J. van Kranendonk, and K. Compaan, Physica 16, 545 (1950).
8. K. A. Brueckner and J. L. Gammel, Phys. Rev. 109, 1023 (1958).
9. R. D. Puff, Ann. Phys. (N. Y.) 13, 317 (1961).
10. Bethe [H. A. Bethe, Phys. Rev. 138, B804 (1965)] has found that in nuclear matter three-body clusters produce important effects, and, since the range of the potential is of the same size as the interparticle spacing in nuclear matter and about twice the interparticle spacing in liquid He^3, we would expect these terms to be even more important in He^3. A crude estimate of the contribution can be

obtained by leaving out all three-body effects (which has been found to be the best way to proceed with a two-particle correlation calculation in nuclear matter); that is, by using G_0 in Eq. (47). We obtain an average energy per particle of $\sim -2^{\circ}K$ at an interparticle separation of $r_0 < 2.25$ Å (compare Table I). Certainly, quantitative agreement with experiment will require that some attention be devoted to three-body cluster.

Pitaevskii [L. P. Pitaevskii, Soviet Phys. JETP 37(10), 1267 (1960); see also L. P. Gorkov and L. P. Pitaevskii, Soviet Phys. JETP 42(15), 417 (1962)] has found a large shielding effect in liquid He^3 for high angular momentum states. The binding energy is primarily determined, however, by the low angular momentum states and we would consequently expect that the shielding will not be an important quantitative correction.

For a "normal" system we may expect that these corrections will have only a small effect on the general features of the spectral function --which is the primary object of study in this paper.

11. G. Baym, Phys. Rev. 127, 1391 (1962). See also G. Baym and L. P. Kadanoff, Phys. Rev. 124, 287 (1961).

12. We use units throughout this paper in which $m = \hbar = 1$; however, we generally include m explicitly.

13. Actually we should use the microcanonical average,

$$[N\,E\,|X|\,N\,E] = \frac{\sum_{\xi} \langle N\,E\,\xi\,|X|\,N\,E\,\xi\rangle}{\sum_{\xi} \langle N\,E\,\xi\,|\,N\,E\,\xi\rangle},$$

where $|NE\xi\rangle$ is an N particle state with total energy E and the other constants of motion needed to specify the state are denoted by ξ. However, Martin and Schwinger[2] have shown that this average is approximately equal to the canonical average (Eq. 6).

14. L. D. Landau and E. M. Lifshitz, Statistical Physics (Pergamon Press Ltd., London-Paris, 1958).

15. L. P. Kadanoff and G. Baym, Quantum Statistical Mechanics (W. A. Benjamin, New York, 1962).

16. N. M. Hugenholtz and L. Van Hove, Physica 24, 363 (1958).

17. We make use of the standard abbreviation

$$(1) = (\underset{\sim}{r}_1, t_1), \qquad (1') = (\underset{\sim}{r}_1', t_1'), \quad \text{etc.}$$

18. G. Baym and N. D. Mermin, J. Math. Phys. 2, 232 (1961).

19. J. A. Shohat and J. D. Tamarkin, The Problem of Moments (American Mathematical Society, New York, 1943). This theorem is Lemma 2.2 on page 24. (The authors wish to thank Dr. R. L. Omnes for a discussion concerning this theorem and for bringing this proof to their attention.)

20. J. M. Luttinger, Phys. Rev. 121, 942 (1961).

21. K. M. Watson, Phys. Rev. 103, 489 (1956).

22. F. Riesz and B. Sz-Nagy, Functional Analysis (Frederick Ungar, New York, 1955); see Section 69.

23. Z. Kopal, Numerical Analysis (John Wiley and Sons, Inc., New York, 1961).

24. R. H. Sherman and F. J. Edeskuty, Ann. Phys. (N. Y.) 9, 522 (1960).

25. D. S. Falk and L. Wilets, Phys. Rev. 124, 1887 (1961).

26. Brueckner and Goldman [K. A. Brueckner and D. T. Goldman, Phys. Rev. 117, 207 (1960)] discuss the modification of the single-particle energy necessary to maintain the Hugenholtz-Van Hove theorem in this calculation. Brueckner, Gammel, and Kubis [K. A. Brueckner, J. L. Gammel, and J. T. Kubis, Phys. Rev. 118, 1438 (1960)] have redone the nuclear matter calculation of Brueckner and Gammel, using a modified single-particle energy, and they find that the Hugenholtz-Van Hove theorem is almost satisfied in this calculation. Masterson and Sawada [K. S. Masterson, Jr., and K. Sawada, Phys. Rev. 133, A1234 (1964)] state that the Hugenholtz-Van Hove theorem is not applicable to reaction matrix calculations.

27. E. C. Kerr, Phys. Rev. 96, 551 (1954).

28. V. J. Emery, Ann. Phys. (N. Y.) 28, 1 (1964).

29. C. C. Sung (Lawrence Radiation Laboratory), private communication, 1964.

30. L. I. Schiff, Quantum Mechanics (McGraw-Hill Book Co., Inc., New York, 1955).

31. The spherical Hankel transform of $g(r)$ is given by

$$g(p) = 4\pi \int_0^\infty r^2 \, dr \, j_\ell(pr) \, g(r) \, .$$

Table I. Primary quantities, present calculation, other calculations, experiment (T = 0). The calculated values of the chemical potential are the solution of Eq. (53). The common temperature units with $\kappa = 1$ for energy are used; the conversion factor for the units used in the figures is $1\ \text{Å}^{-2} = 16.36$ degrees.

Source (and reference number)	Average energy per particle, $\langle E/N \rangle$ (°K)	Chemical potential, μ (°K)	Interparticle separation, r_0 (Å)	Effective mass, m^*/m
Experimental	-2.53 [a]	-2.53 [a]	2.43 [c]	2.15 [d]
Mills, 5	0.0	0.0	5.60	
Sung, 4	-2.8	-	-	≈ 2.7
Puff-Martin approximation, 1	-0.043	-0.811	3.25	1.0
Brueckner and Gammel, 3	-0.96	-3.61 [b]	2.60	1.84
$\langle T \rangle_0$ Calculation	-1.16	-1.39	2.47	

a. Ref. 24
b. Ref. 26
c. Ref. 27
d. Ref. 28

UCRL-16524

Table II. Parameters and deviations, Eq. (A.6), for separable potentials fitted to the Lennard-Jones and Yntema-Schneider potentials.

Potential	ℓ	r_c	β	$g_\ell^{(2)}$ [a]	$(\mathrm{Dev})_\ell$
Lennard-Jones	0	1.872	1.505	-0.00805	0.019
	1	1.908	1.635	-0.00818	0.030
	2	1.857	1.421	-0.0713	0.042
	3	1.73	0.0	-0.475	0.103
	4	1.0	0.8285	-1.347	0.057
	5	1.0	0.9573	-1.038	0.058
	6	1.0	0.897	-1.686	0.034
Yntema-Schneider	0	2.048	1.023	-0.000947	0.014
	1	2.050	0.977	-0.00218	0.031
	2	2.085	0.855	-0.0161	0.039
	3	1.997	0.0	-0.0518	0.221
	4	1.0	0.621	-4.76	0.790
	5	1.0	0.781	-2.25	0.185
	6	1.0	1.014	-1.29	0.033

a. $g_\ell^{(1)} \approx -10^{-4}\, g_\ell^{(2)}$

FIGURE CAPTIONS

1. Diagrams for ϕ and Σ. The solid lines represent G and the dotted lines V.
   (a) ϕ in the Hartree-Fock approximation;
   (b) Σ in the Hartree-Fock approximation;
   (c) a term in ϕ for the TCTM approximation;
   (d) the term in Σ corresponding to the term illustrated in (c).
2. The real part of R (Eq. 46) for representative values of momentum ($\langle T \rangle_0$ approximation). Dashed lines are at poles in $\langle T \rangle_0$ and dotted lines are smooth values of R used in calculation.
3. The imaginary part of R (Eq. 46) for representative values of momentum ($\langle T \rangle_0$ approximation).
4. Iterations of the single-particle energy (Eq. 50) for $\langle T \rangle_0$ approximation. The zeroth approximation is the kinetic energy minus $p_f^2/2m$, and the dotted line is the ninth iteration.
5. $\epsilon(p,\omega)$ (Eq. 49) for a representative value of p_f and p near p_f. The dotted line is $\epsilon = \omega$, whose intersection with $\epsilon(p,\omega)$ gives $\epsilon(p)$ (Eq. 50).
6. The single-particle energy, $\epsilon(p)$. The solid line is the $\langle T \rangle_0$ approximation and the dotted line is $\epsilon(p) = (p^2 - p_f^2)/2m$.
7. $\epsilon(p,\omega)$ (Eq. 49) for representative values of momentum.
8. $\Gamma(p,\omega)$ (Eq. 47b), the imaginary part of the self-energy for representative values of momentum. (a) ω near zero [$\Gamma(p,\omega) \to \infty$ as $\omega \to -\infty$], (b) $\omega > 0$.

9. Momentum density distribution function (Eq. 54); (a) $p < p_f$, (b) $p > p_f$. (Note change in scales.)
10. The width function (Eq. 51) (the curve approaches unity for large momentum).
11. Average energy per particle and chemical potential versus density for the Puff-Martin approximation (Ref. 1).
12. Average energy per particle (Eq. 57) and chemical potential (Eq. 53) versus density (Eq. 56). Here e_{T_0} and μ_{T_0} are obtained from the $\langle T \rangle_0$ approximation, and e_E and μ_E from the experimental values obtained by extrapolating the data of Ref. 24 to zero degrees.
13. Density versus Fermi momentum; solid line is the $\langle T \rangle_0$ approximation and dotted line the ideal Fermi gas density.
14. Presure versus density ($\langle T \rangle_0$ approximation). Curve 1 is obtained by using Eq. (10), and curve 2 by using Eq. (12). The experimental curve (dotted) is an extrapolation of the data of Ref. 24.

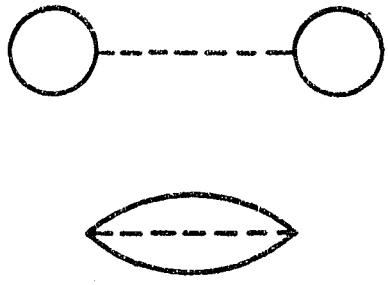

(a)

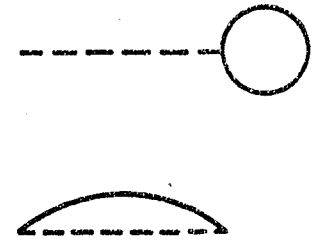

(b)

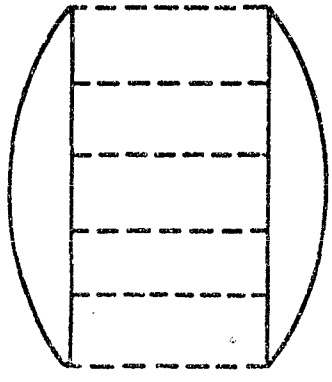

(c)

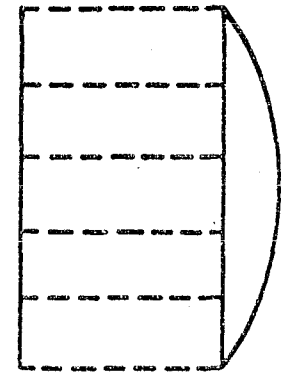

(d)

Fig. 1

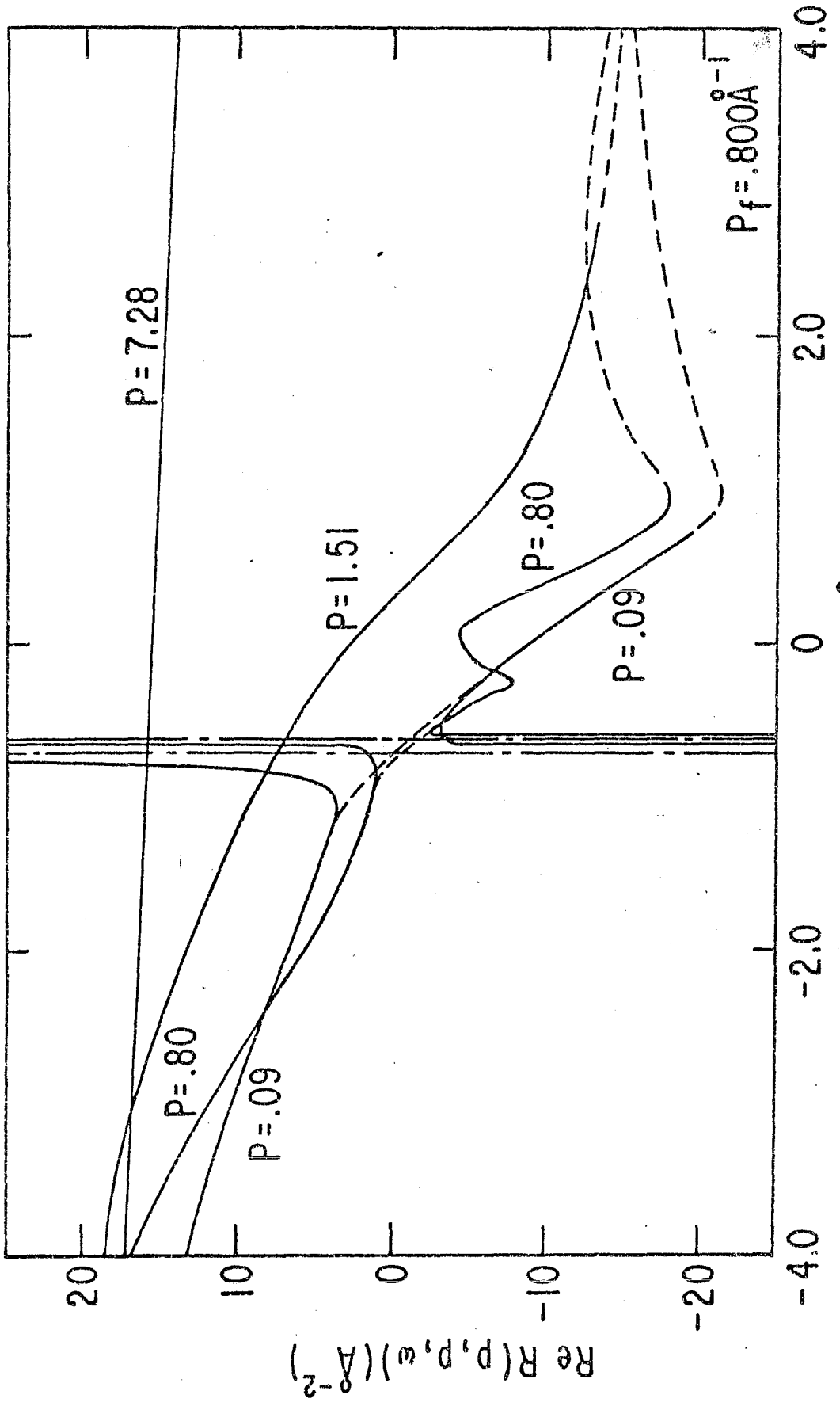
P=7.28
P=1.51
P=.80
P=.09
P=.80
P=.09
P_f=.800Å^{-1}
Re R(p,p,ω)(Å^{-2})
ω(Å^{-2})
20
10
0
-10
-20
4.0
2.0
0
-2.0
-4.0

Fig. 2

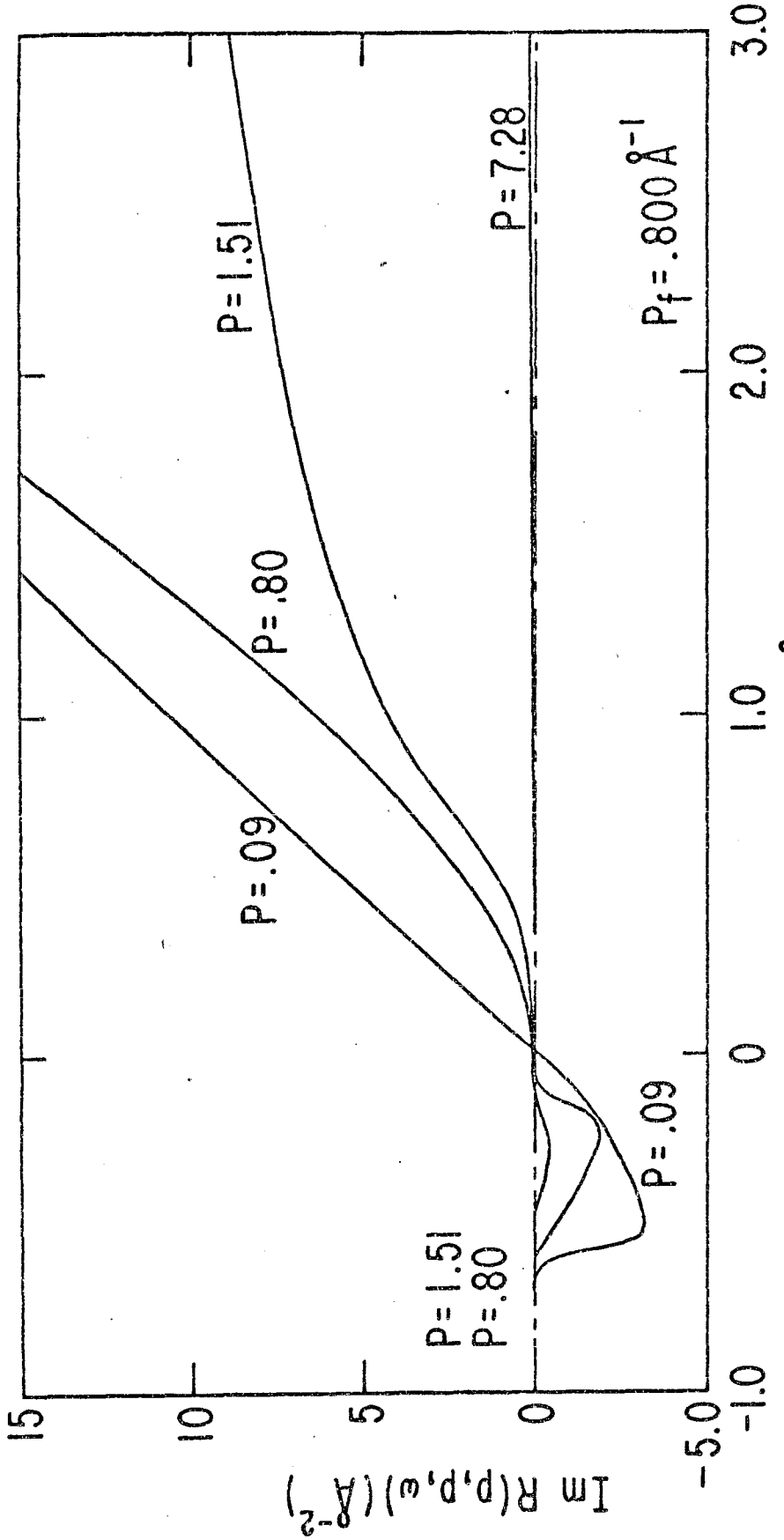
Im R(p,p,ω)(Å⁻²)
15
10
5
0
-5.0
-1.0
0
1.0
2.0
3.0
ω (Å⁻²)
P=1.51
P=.80
P=.09
P=7.28
P=1.51
P=.80
P=.09
Pf=.800 Å⁻¹

Fig. 3

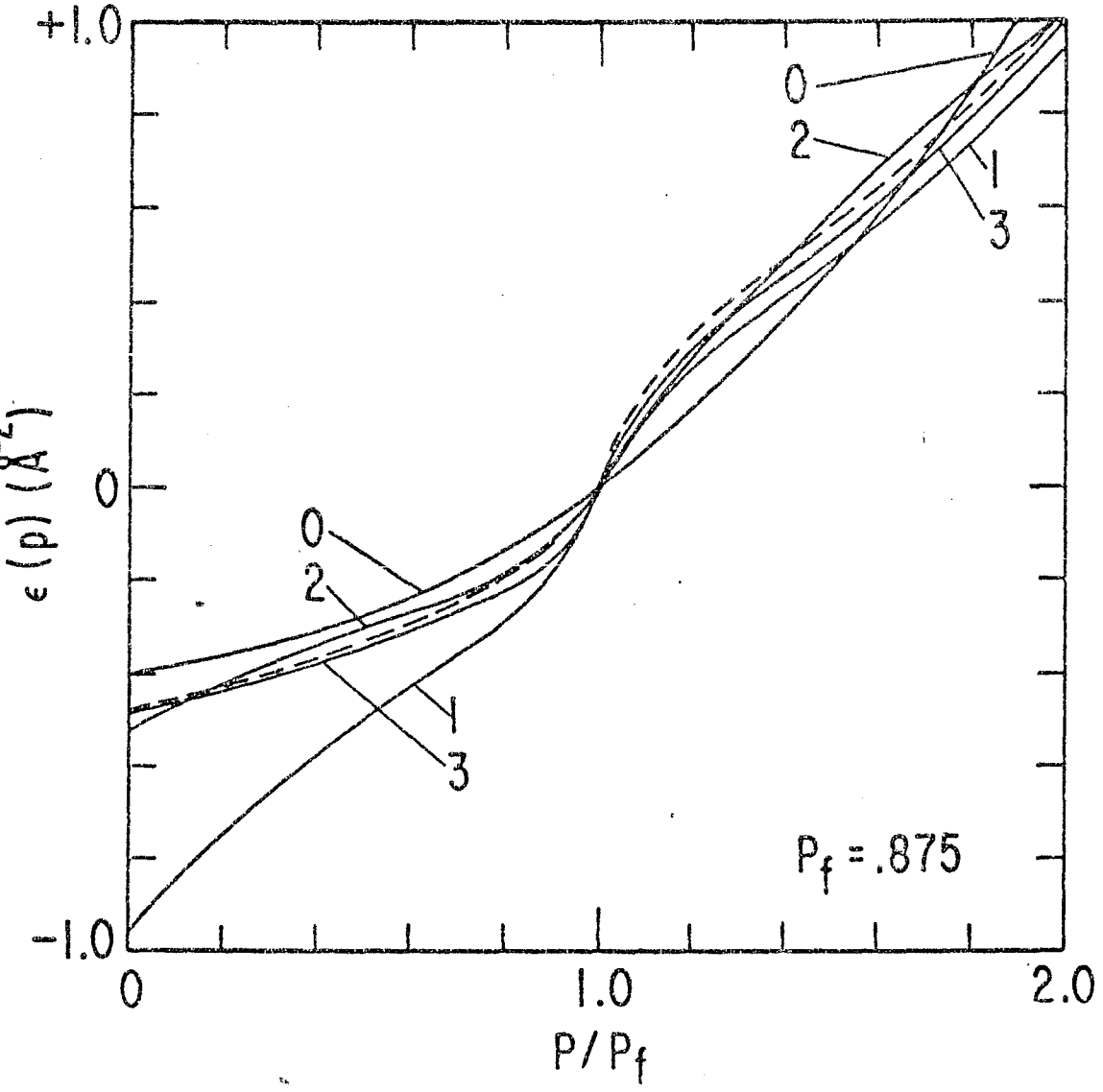

Fig. 4

FIG 4

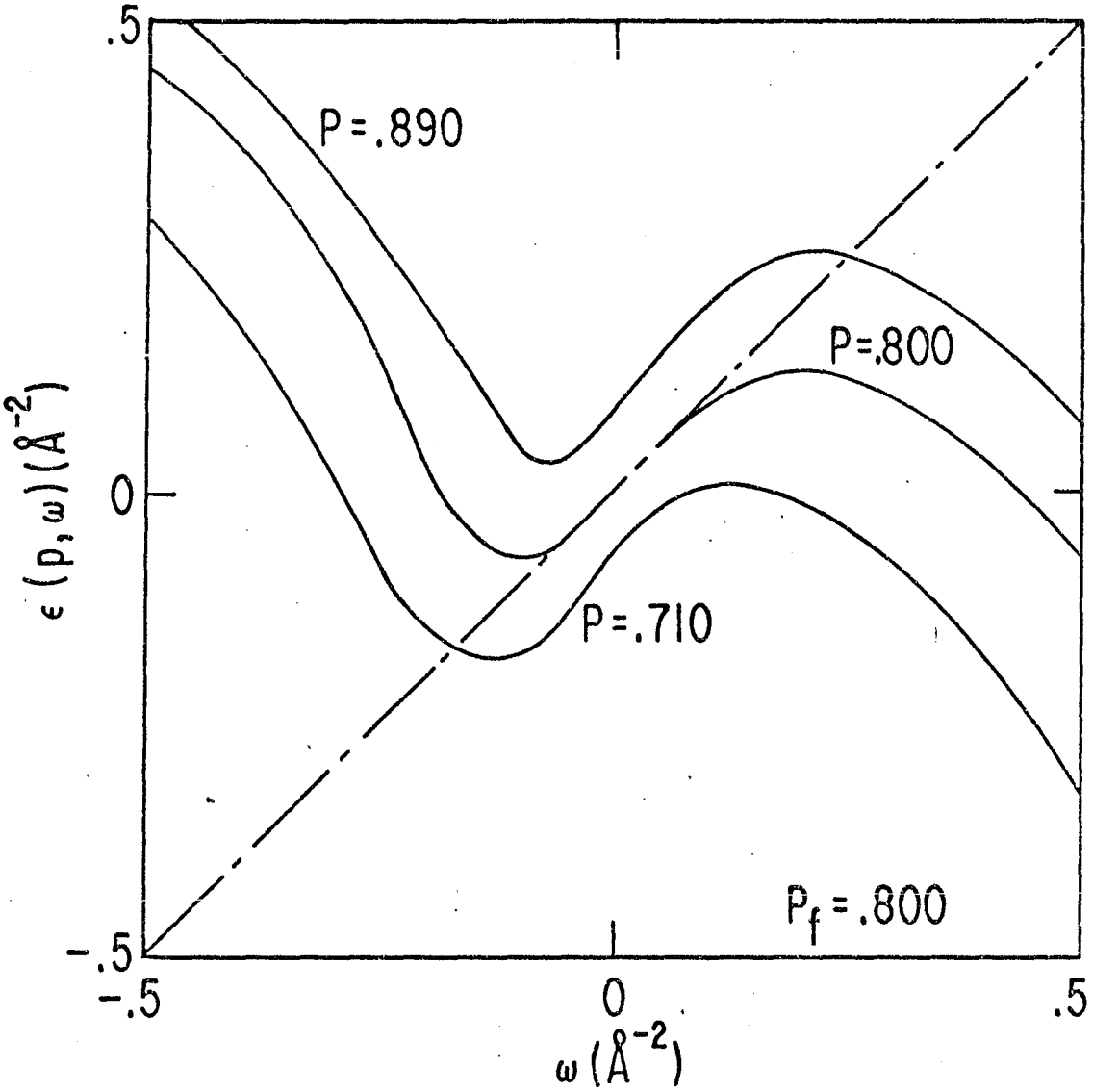

Fig. 5

FIG 5

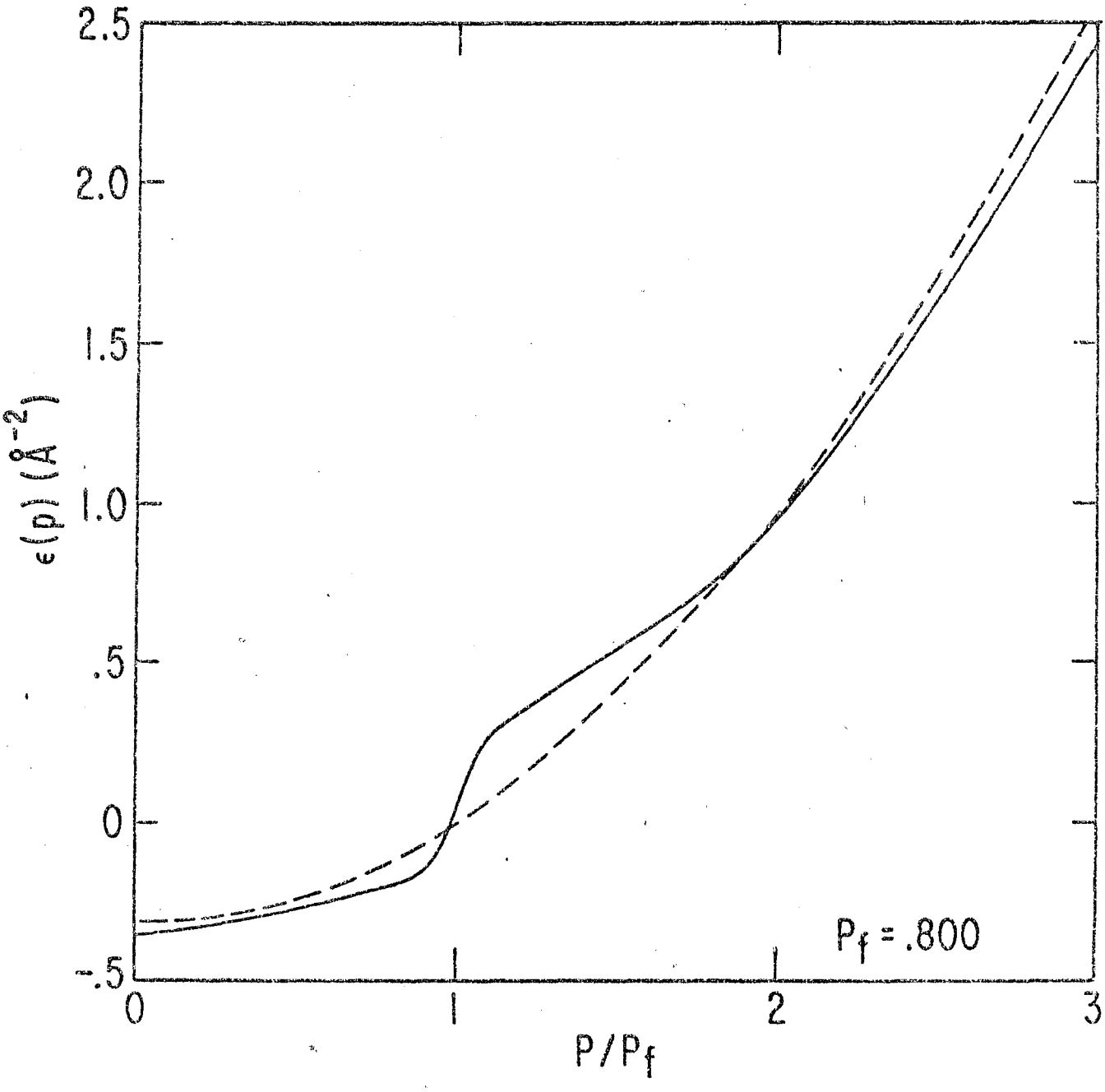

Fig. 6

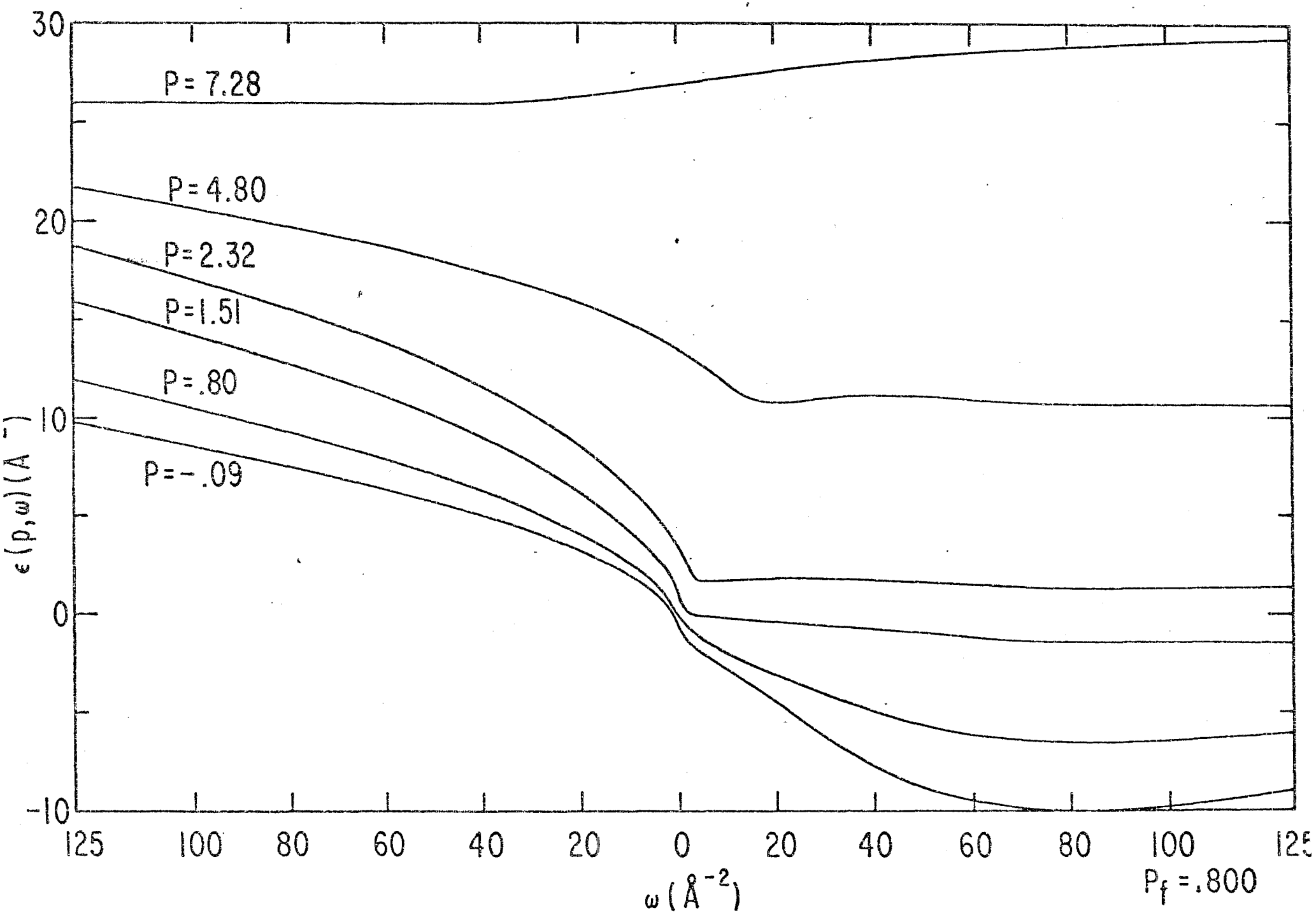
30
20
10
0
-10
P = 7.28
P = 4.80
P = 2.32
P = 1.51
P = .80
P = - .09
ε (p, ω) (Å⁻¹)
125
100
80
60
40
20
0
20
40
60
80
100
125
ω (Å⁻²)
Pf = .800

Fig. 7

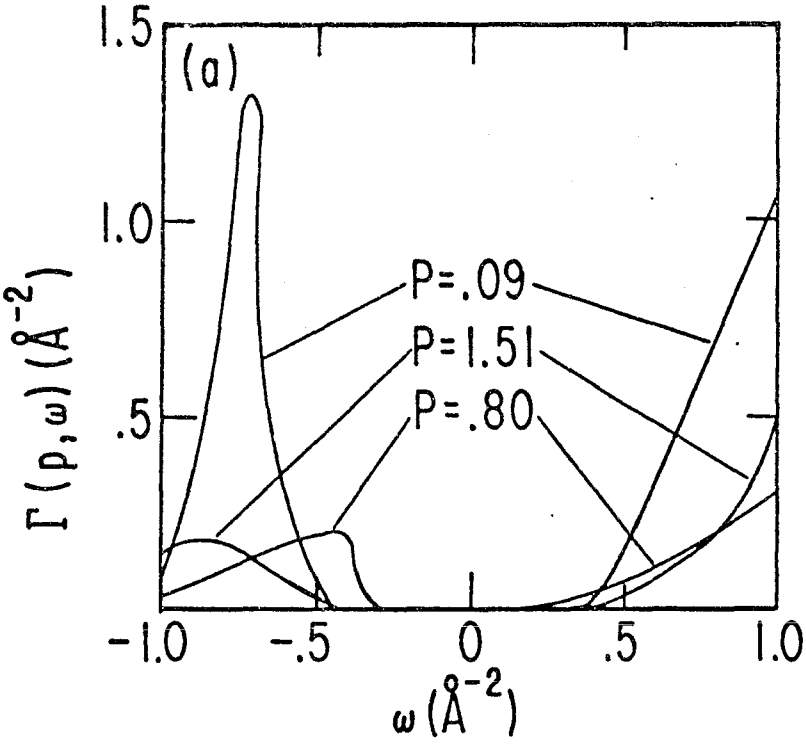
(a)
P=.09
P=1.51
P=.80
Γ(p,ω) (Å⁻²)
ω (Å⁻²)
1.5
1.0
.5
-1.0
-.5
0
.5
1.0

FIG 8 (a)

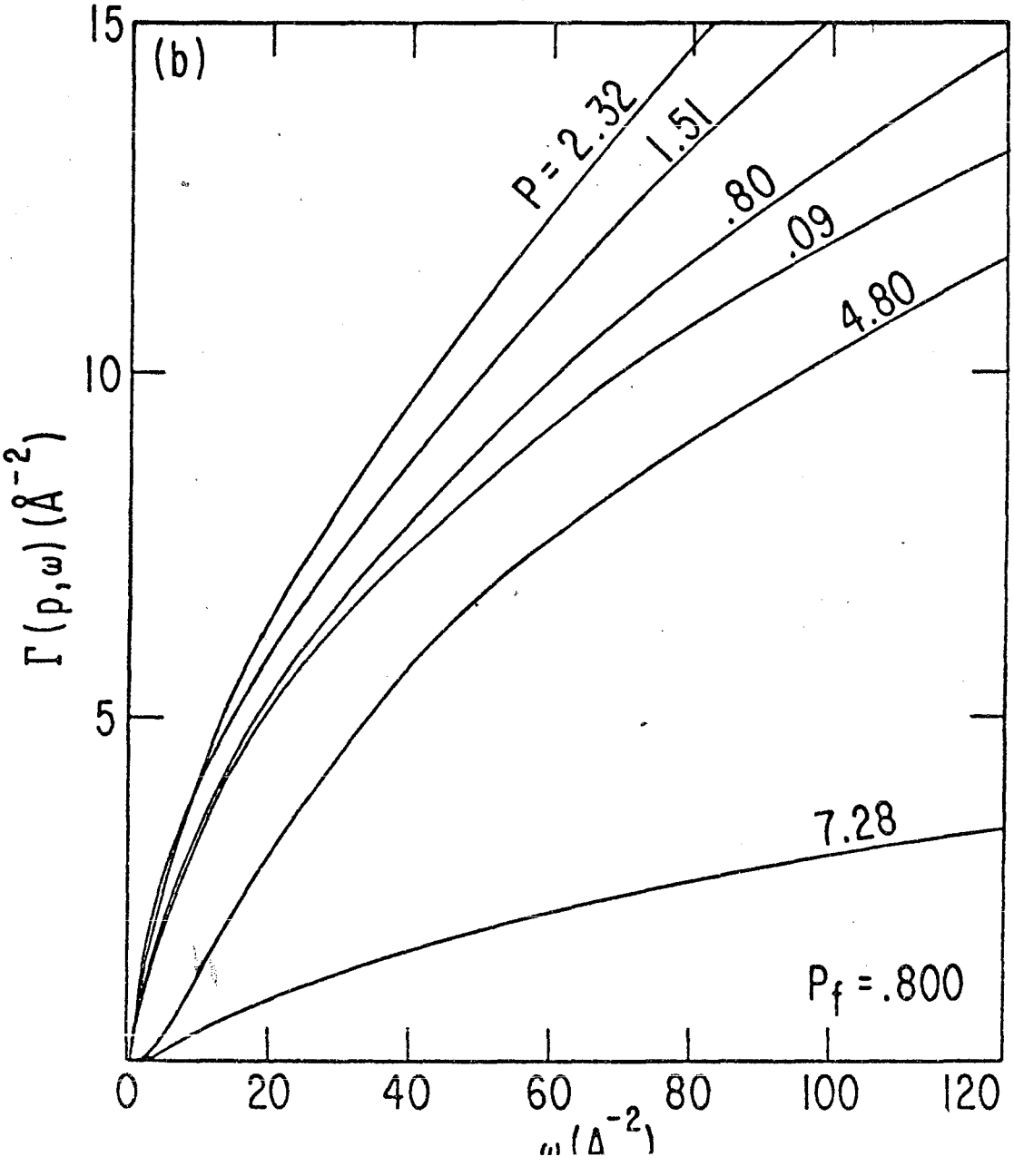
(b)
P=2.32
1.51
.80
.09
4.80
7.28
P_f = .800
Γ(p,ω) (Å⁻²)
ω (Å⁻²)
15
10
5
0
20
40
60
80
100
120

FIG 8 (b)

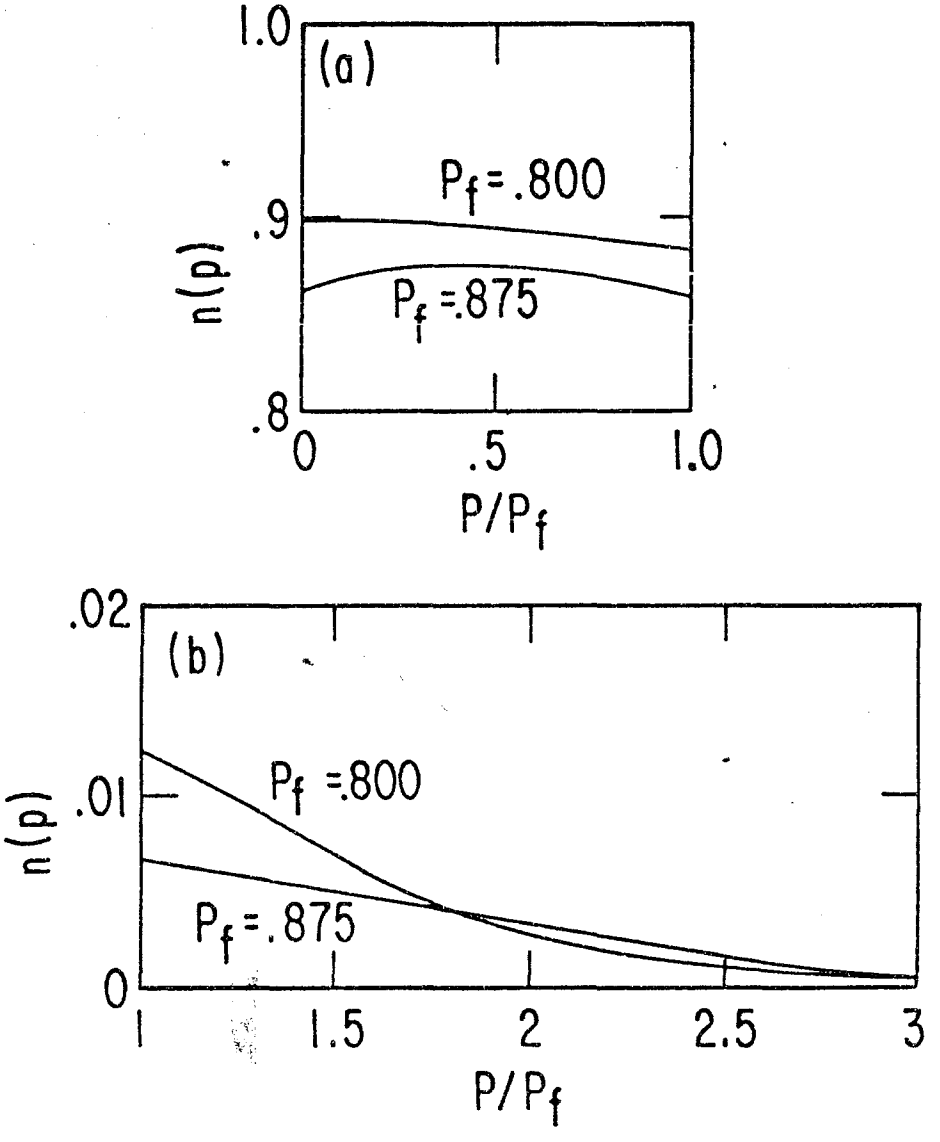
1.0
(a)
P_f = .800
.9
n(p)
P_f = .875
.8
0
.5
1.0
P/P_f
.02
(b)
P_f = .800
.01
n(p)
P_f = .875
0
1
1.5
2
2.5
3
P/P_f

Fig. 9

FIG 10

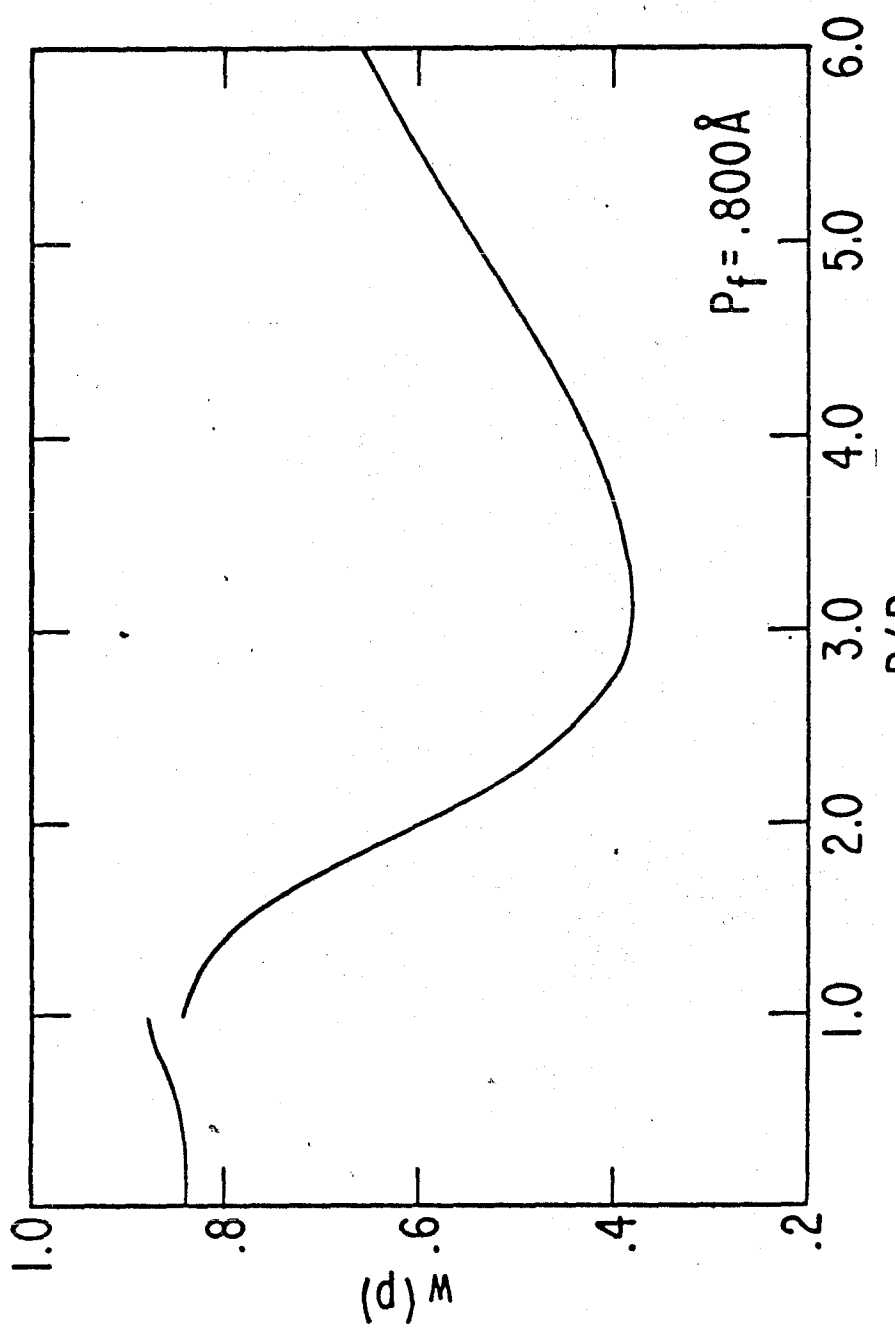

Fig. 10

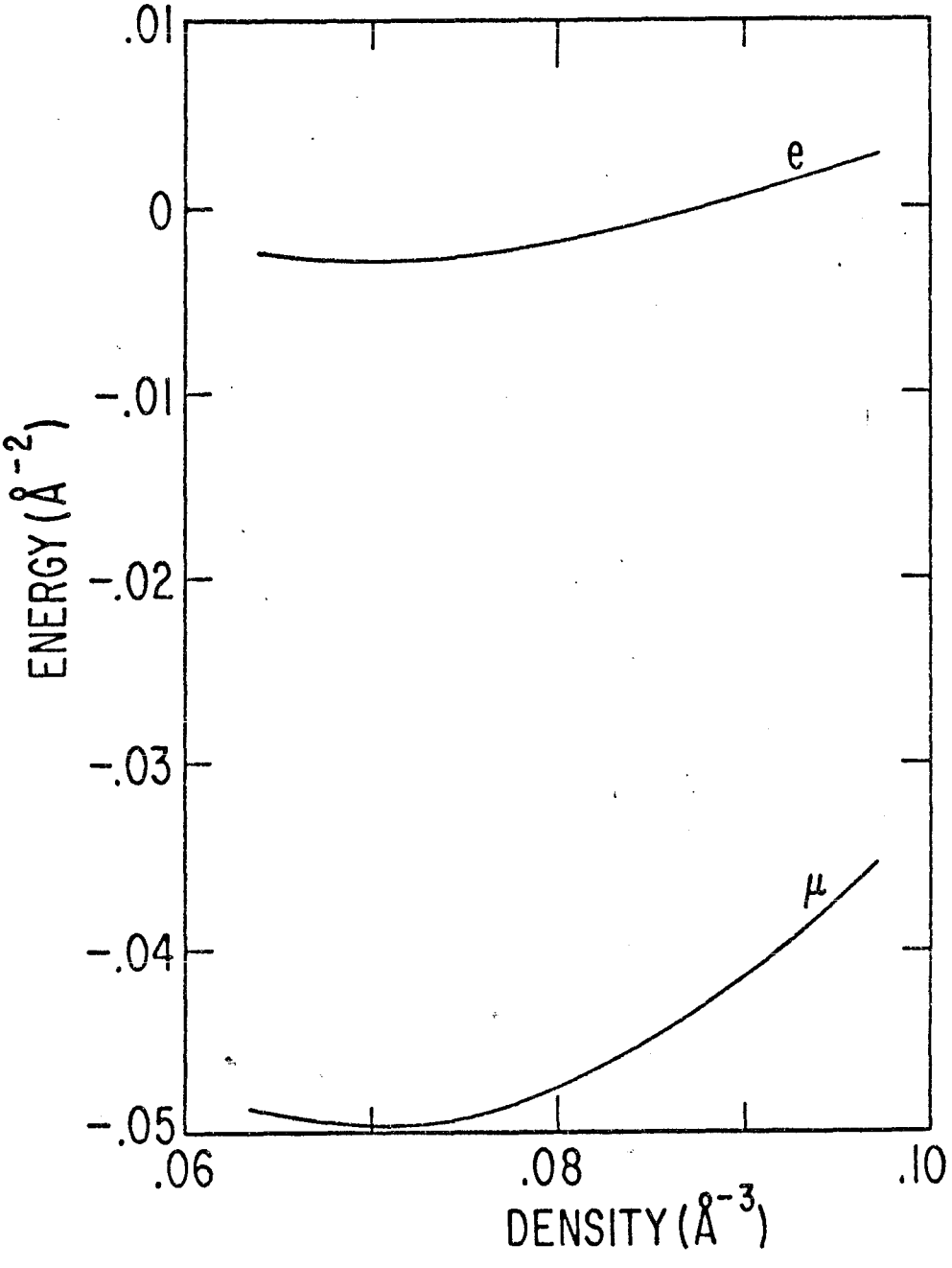

Fig. 11

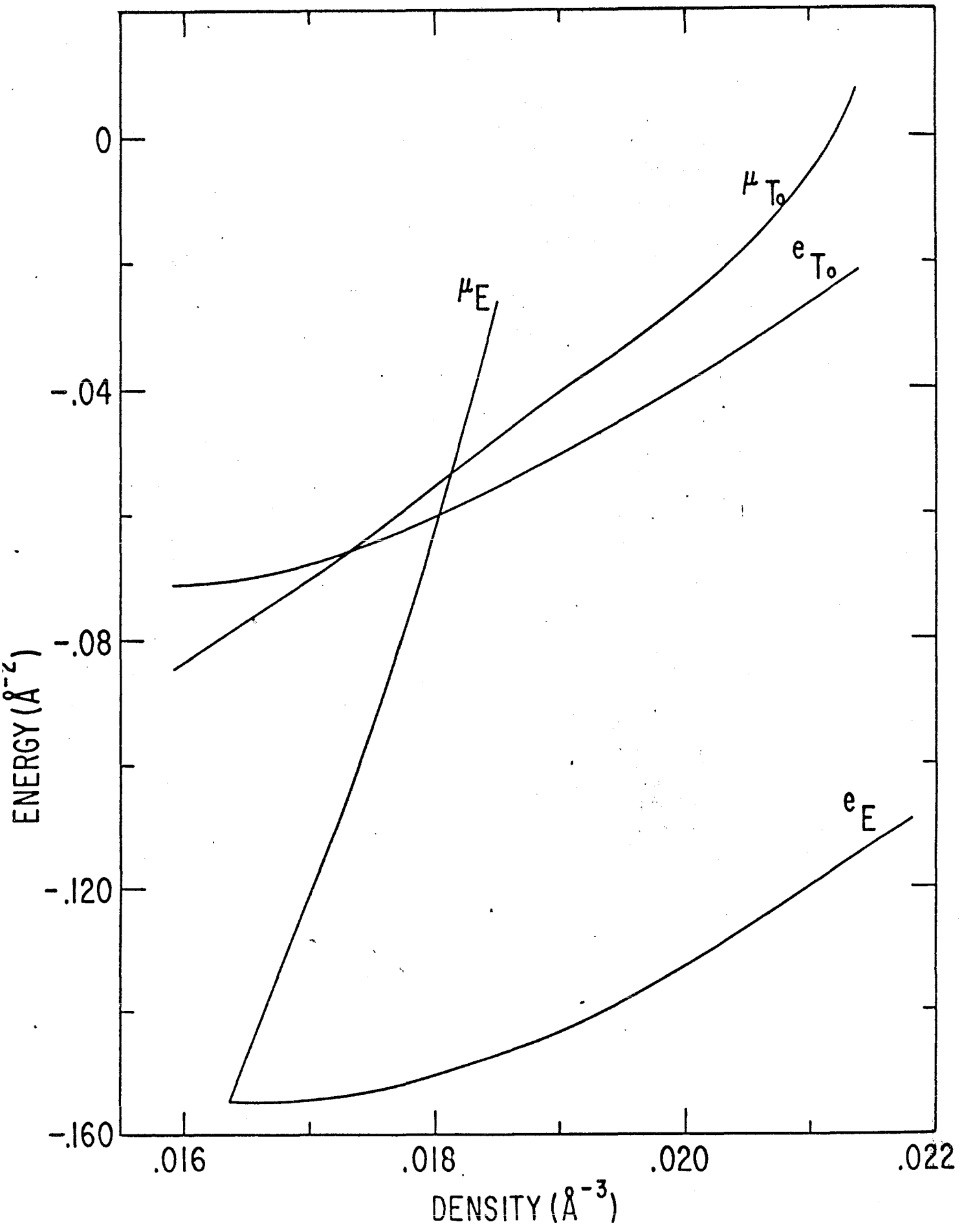
0
-.04
-.08
-.120
-.160
ENERGY (Å^{-2})
.016
.018
.020
.022
DENSITY (Å^{-3})
μ_{T_o}
e_{T_o}
μ_E
e_E

Fig. 12

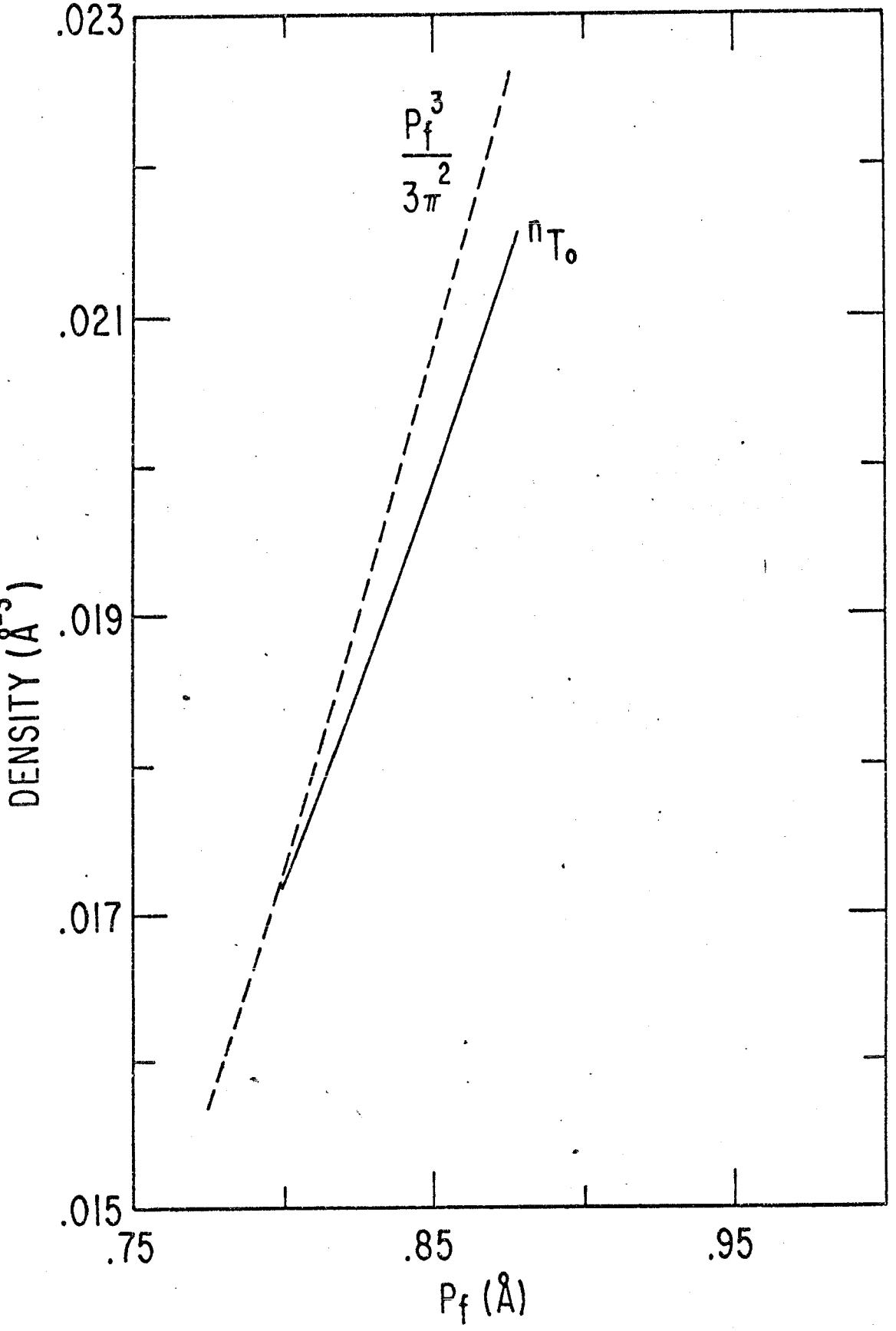
.023
.021
.019
.017
.015
DENSITY (Å^{-3})
$\frac{P_f^3}{3\pi^2}$
$\bar{n}T_0$
.75
.85
.95
P_f (Å)

Fig. 13

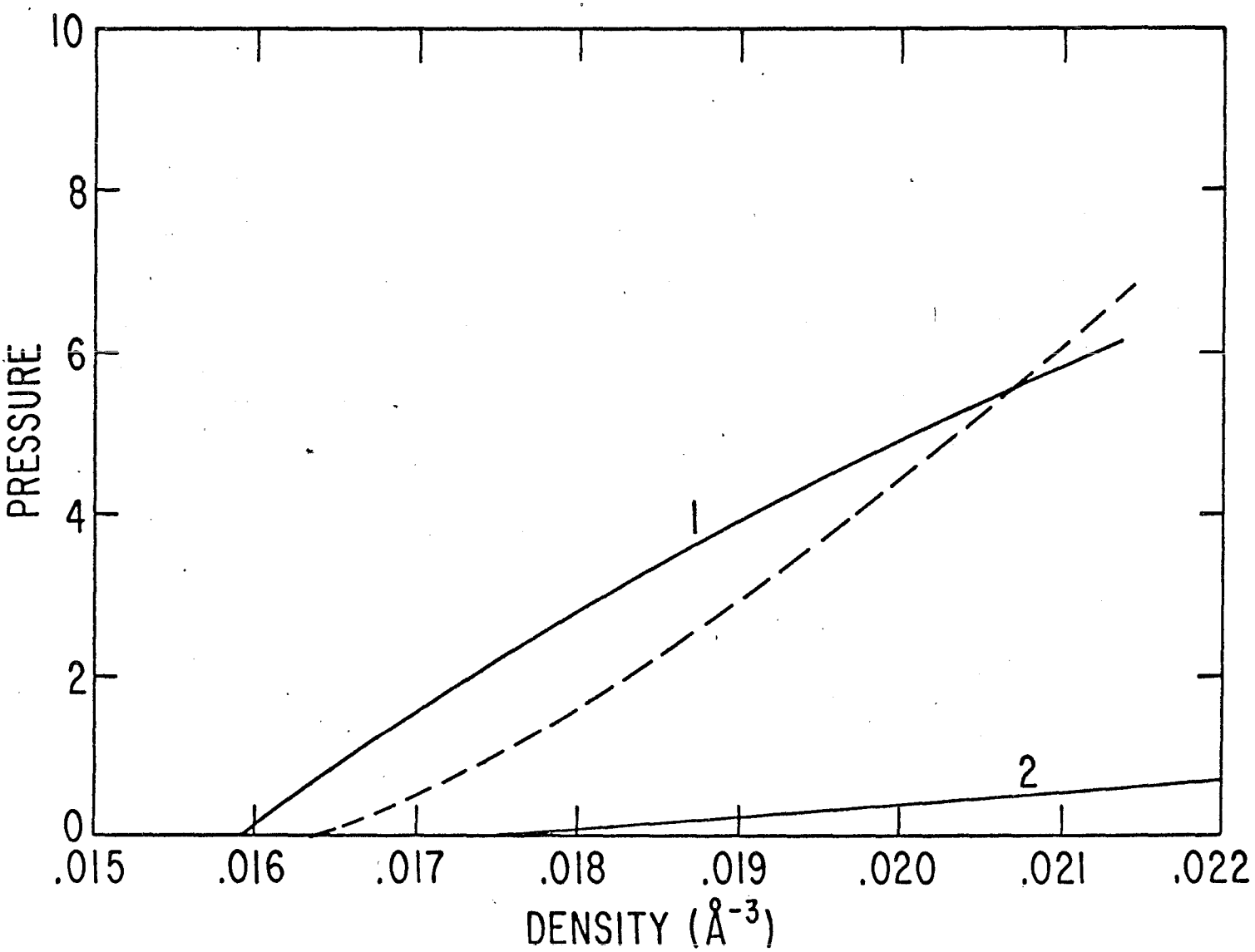
10
8
6
4
2
0
PRESSURE
1
2
.015
.016
.017
.018
.019
.020
.021
.022
DENSITY (Å^{-3})

Fig. 14